STRUCTURAL HEALTH MONITORING CONDITION ASSESSMENT AND SEISMIC VULNERABILITY ESTIMATION OF HIGHWAY BRIDGES

by

Hüseyin Çolak

B.S., Civil Engineering, Boğaziçi University, 2013

Submitted to the Institute for Graduate Studies in
Science and Engineering in partial fulfillment of
the requirements for the degree of
Master of Science

Graduate Program in Civil Engineering

Boğaziçi University

2016

STRUCTURAL HEALTH MONITORING CONDITION ASSESSMENT AND SEISMIC VULNERABILITY ESTIMATION OF HIGHWAY BRIDGES

APPROVED BY:

Assoc. Prof. Serdar Soyöz .....
(Thesis Supervisor)

Prof. F. Necati Çatbaş .....

Assoc. Prof. Kutay Orakçal .....

DATE OF APPROVAL: 24.06.2016

to my parents

ACKNOWLEDGEMENTS

I would like to express my greatest appreciation and reverence to my supervisor, Assoc. Prof. Serdar Soyöz, for his leading me into this interesting research area, and offering me this precious opportunity to gain experiences not limited in structural engineering, but also in time management and technical writing. This thesis would not have been possible without his encouragement, guidance and support throughout my graduate study.

I would like to thank my committee members, Prof. Necati Çatbaş for his advice during the last year of my graduate study, and Assoc. Prof. Kutay Orakçal for his attention, time, and valuable suggestions. I am also grateful to Prof. Hilmi Luş for his continuous contributions during my undergraduate and graduate studies and to Assist. Prof. Serdar Selamet who is the supervisor of my undergraduate project.

I am also thankful to TÜBİTAK (Scientific and Technological Research Council of Turkey) who funded this study via project 11M436 and to KGM (General Directorate of Highways) who supported me during the selection, instrumentation and monitoring of Etiler Bridge.

I should also thank my talented research mates, Oğuz Şenkardeşler and Korkut Kaynardağ, who have kindly helped me in this journey and Oğuz's brother Burak Şenkardeşler for his support during the preparation of bridge drawings.

Thanks are also owed to my dear friends, Melih Akar, İbrahim Uzun, Noyan Renda, Mustafa Boran and Rıdvan Kanbaş for their invaluable friendship and support since my first days in the university.

Last but not least, I would like to show my deepest appreciation to my parents for their unconditional love and emotional encouragement throughout my life.

ABSTRACT

STRUCTURAL HEALTH MONITORING CONDITION ASSESSMENT AND SEISMIC VULNERABILITY ESTIMATION OF HIGHWAY BRIDGES

Seismic vulnerability estimation is one of the crucial targets of performance evaluation and risk assessment strategies in structural engineering and it is widely achieved by developing fragility and/or capacity curves using analytical models of structures. Since the accuracy of finite element models and analysis results has a key role in the evaluation of existing structures, this study focuses on two important factors affecting the accuracy of models and analyses results. The first one is structural condition and the second factor is the nonlinear modelling of structural elements. Conventional practices of condition assessment rely on visual inspection. However, it is well-known that to have a quick and reliable visual-based assessment is almost impossible due to several limitations such as subjective judgement of a damage and unreachable locations of huge structures. On the other hand, structural health monitoring can revolutionize the way of condition assessment in a rapid and objective way. For this purpose, implementation of vibration-based monitoring and system identification of reinforced concrete bridges is presented. An ordinary highway bridge in Istanbul is instrumented with acceleration sensors and vibration measurements are used to calibrate the finite element model of the bridge developed according to design drawings. Afterwards, measurements of a large scale bridge experiment carried out at University of Nevada-Reno is used to validate the proposed condition assessment method by comparing the identified stiffness values with ones calculated using curvature measurements. Moreover, effects of nonlinear modelling on condition assessment and seismic vulnerability estimation were investigated by nonlinear time history analyses carried out using two hinge models.

ÖZET

KARAYOLU KÖPRÜLERİNİN YAPI SAĞLIĞI İZLEMESİ YAPISAL DURUM DEĞERLENDİRMESİ VE SİSMİK GÜVENİLİRLİK TAHMİNİ

Sismik güvenilirlik tahminleri, yapısal performans ve risk değerlendirmesi stratejilerinde kullanılan en önemli araçlardan biridir. Güvenilirlik tahminleri yapıların sonlu eleman modelleri kullanılarak oluşturulan kırılganlık ve kapasite eğrilerine dayandığını için modellerin ve analiz sonuçlarının gerçeğe uygun olması, mevcut yapıların değerlendirilmesinde kilit rol oynamaktadır. Bu çalışmada sonlu eleman modelleri ve analiz sonuçlarının doğruluğunu belirleyen iki konu incelenmektedir. Bunlardan ilki yapısal durum değerlendirmesi iken diğeri yapıların doğrusal olmayan davranışlarının modellenmesidir. Geleneksel yapısal durum değerlendirmesi yöntemi olan görsel inceleme ile hem hızlı hem de güvenilir sonuçlar almanın hemen hemen imkânsız olduğu bilinmektedir. Bu nedenle, bu çalışma kapsamında titreşim ölçümlerinin kullanılmasına dayanan bir yapısal durum değerlendirmesi yöntemi sunulmaktadır. Bu bağlamda, İstanbul'da bulunan bir karayolu köprüsünün ivme-ölçerler ile enstrümantasyonu gerçekleştirilmiştir. Daha sonra köprünün tasarım çizimleri kullanılarak sonlu eleman modeli oluşturulmuş ve bu model ivme ölçümlerinin modal analizinden elde edilen sonuçlar kullanılarak kalibre edilmiştir. Çalışma kapsamında önerilen yöntemin doğrulanması ise Nevada Üniversitesi'nde gerçekleştirilen büyük ölçekli köprü deneylerinin ölçümlerinden yararlanılarak gerçekleştirilmiştir. Deneyde test edilen köprü aynı zamanda bu çalışma kapsamında yapıların doğrusal olmayan davranışının modellenmesi üzerine yapılan incelemelerde de kullanılmıştır. Çalışmanın bu bölümünün amacı ise farklı modelleme yöntemleri kullanılarak oluştutulan köprünün doğrusal olmayan analitik modelleri kullanılarak elde edilen yapısal durum değerlendirmesi ve sismik güvenilirlik tahmini sonuçlarındaki farklılıkların belirlenmesi.

TABLE OF CONTENTS

ACKNOWLEDGEMENTS iv
ABSTRACT v
ÖZET vi
LIST OF FIGURES ix
LIST OF TABLES xii
LIST OF SYMBOLS xv
LIST OF ACRONYMS/ABBREVIATIONS xvii
1. INTRODUCTION 1
1.1. Objective 1
1.2. Literature Review 2
1.2.1. Structural Health Monitoring 2
1.2.2. System Identification 3
1.2.3. Damage Detection 5
1.2.4. Bridges 9
1.2.5. Reliability Estimation 16
1.2.6. Nonlinear Modelling 18
1.3. Thesis Outline 20
2. DESCRIPTION OF BRIDGE, MONITORING SYSTEM AND VIBRATION MEASUREMENTS 21
2.1. Etiler Bridge and Monitoring System 21
2.1.1. Long-Term Monitoring System 22
2.1.2. Short-Term Monitoring System 25
2.2. Vibration Measurements and Long-Term Database 26
3. SYSTEM IDENTIFICATION AND FINITE ELEMENT MODEL UPDATING OF THE BRIDGE 29
3.1. Design Drawings and Initial Finite Element Model 29
3.1.1. Simplified Model of the Bridge 29
3.1.2. Modelling of the Abutments 32
3.1.3. Modelling of Footings 36

3.2. System Identification 37
4. CONDITION ASSESSMENT AND SEISMIC VULNERABILITY ESTIMATION OF A FOUR-SPAN BRIDGE MODEL 43
4.1. Experimental Setup and Test Procedure 43
4.2. Finite Element Modelling and Nonlinear Analysis 46
4.3. System Identification and Finite Element Model Updating 51
4.4. Identified and Predicted Damage Progress 56
4.5. Seismic Vulnerability Estimation 59
5. CONCLUSION 65
REFERENCES 67

LIST OF FIGURES

Figure 2.1. Location of the bridge. 21

Figure 2.2. Etiler bridge. 22

Figure 2.3. Sensor layout of the bridge. 23

Figure 2.4. Sensors located at the ground level. 23

Figure 2.5. Sensors located on the first column. 24

Figure 2.6. Sensors located on the second column. 24

Figure 2.7. Short-term monitoring of the third column. 25

Figure 2.8. Short-term monitoring of the third span. 25

Figure 2.9. Vibration measurements in the transverse direction: (a) to (c) show Bent-1 to Bent-3. 27

Figure 2.10. Vibration measurements in the vertical direction: (a) to (d) show Span-1 to Span-4. 27

Figure 2.11. First modal frequency in the transverse direction. 28

Figure 2.12. First modal frequency in the vertical direction. 28

Figure 3.1. Top view of the bridge. 30

Figure 3.2. Elevation view of the deck (unit is cm). 30

Figure 3.3. Top view of the columns (unit is cm). 30

Figure 3.4. Elevation view of the columns (unit is cm). 31

Figure 3.5. The simplified finite element model of the bridge. 31

Figure 3.6. Side view of abutments (unit is cm). 33

Figure 3.7. Top view of abutments (unit is cm). 33

Figure 3.8. Finite element model with abutments using frame elements. 35

Figure 3.9. Finite element model with abutments using shell elements. 35

Figure 3.10. Finite element model of the bridge developed according to design drawings. 37

Figure 3.11. Power Spectral Density of the Bridge in the Transverse Direction. 38

Figure 3.12. Power Spectral Density of The Bridge In The Vertical Direction. . 39

Figure 3.13. Mode Shapes of the Structure obtained from System Identification and Updated Finite Element Model. 42

Figure 4.1. Test Setup. 44

Figure 4.2. Dimensions of the Bridge. 44

Figure 4.3. Test Procedure: (a) Transverse Direction, (b) Longitudinal Direction. 45

Figure 4.4. The Cross-Sectional Properties and P-M Interaction of Columns. . 46

Figure 4.5. Fiber Hinge Model and Moment-Rotation Response (Test-2). . . . 47

Figure 4.6. Identified Mode Shapes of the Bridge under Test-1. 47

Figure 4.7. Power Spectra of the First Singular Value at Different Damage States. 53

Figure 4.8. Mode Shapes of the Structure obtained from System Identification and Updated FEM. 54

Figure 4.9. Comparison of Identified and Predicted Effective Stiffness. 59

Figure 4.10. Comparison of Fragility Curves at Damage State-1. 63

Figure 4.11. Comparison of Fragility Curves at Damage State-2. 63

Figure 4.12. Comparison of Fragility Curves at Damage State-3. 64

LIST OF TABLES

Table 3.1. Comparison of modal frequencies in the transverse direction obtained by two models. 32

Table 3.2. Comparison of modal frequencies in the transverse direction. . . . 35

Table 3.3. Comparison of modal frequencies in the longitudinal direction. . . 36

Table 3.4. Comparison of modal frequencies in the vertical direction. 36

Table 3.5. Comparison of the frequencies in the transverse direction. 39

Table 3.6. Comparison of the frequencies in the longitudinal direction. 39

Table 3.7. Comparison of the frequencies in the vertical direction. 40

Table 3.8. Comparison of the frequencies in the transverse direction. 41

Table 3.9. Comparison of the frequencies in the longitudinal direction. 42

Table 3.10. Comparison of the frequencies in the vertical direction. 42

Table 4.1. Test Procedure with Ground Motion Levels. 45

Table 4.2. Comparison between Effective Stiffness Values Obtained using Two Hinge Models (Bent-1). 50

Table 4.3. Comparison between Effective Stiffness Values Obtained using Two Hinge Models (Bent-2). 50

Table 4.4. Comparison between Effective Stiffness Values Obtained using Two Hinge Models (Bent-3). 51

Table 4.5. Identified Natural Frequencies. 53

Table 4.6. The Comparison of the Modal Frequencies of the Updated and Non-updated FEMs with Identified ones for Damage State-1 (WN1). . . 55

Table 4.7. The Comparison of the Modal Frequencies of the Updated and Non-updated FEMs with Identified ones for Damage State-2 (WN2). . . 55

Table 4.8. The Comparison of the Modal Frequencies of the Updated and Non-updated FEMs with Identified ones for Damage State-3 (WN3). . . 55

Table 4.9. Comparison of Identified and Predicted Stiffness Values of Bent-1. 56

Table 4.10. Comparison of Identified and Predicted Stiffness Values of Bent-2. 56

Table 4.11. Comparison of Identified and Predicted Stiffness Values of Bent-3. 57

Table 4.12. Comparison of Effective Stiffness of Bent-1 with Damage Levels. . 58

Table 4.13. Comparison of Effective Stiffness of Bent-2 with Damage Levels. . 58

Table 4.14. Comparison of Effective Stiffness of Bent-3 with Damage Levels. . 58

Table 4.15. Rotational ductility limits. 58

Table 4.16. Comparison of Failure Probabilities at Damage State 1. 62

Table 4.17. Comparison of Failure Probabilities at Damage State 2. 62

Table 4.18. Comparison of Failure Probabilities at Damage State 3. 62

LIST OF SYMBOLS

a	Input ground motion
A_e	Effective area of the diaphragm wall
B_F	Width of the Footing
c_i	Mean values of the ith fragility curve
C_L	Effective coefficient of diaphragm wall
C_W	Contribution coefficient
D_f	Depth of the Footing
E	Modulus of elasticity
E_{cj}	Modulus of elasticity
EI	Initial stiffness
EI_{eff}	Effective stiffness
f_{cj}	Compressive strength
f_i	Simulated modal frequency of ith mode
f_i^*	Measured modal frequency of ith mode
g	Gravitational acceleration
h	Height of the diaphragm wall
h_i	Weighing coefficient for ith MAC value
Hz	Heartz
i	Mode Number
I	Moment of inertia
k_i	Weighing coefficient for ith modal frequency
k_s	Coefficient of Soil Reaction
kN	Kilonewton
K_i	Initial stiffness of the backfill
K_l	Longitudinal stiffness of the diaphragm
K_r	Rotation Stiffness Value
K_t	Transverse stiffness of the diaphragm
L_p	Plastic hinge length

mm	Milimeter
M	Moment
M	Magnitude of earthquake
rad	Radian
sec	Second
t	Time
w	Width of the diaphragm wall
α	Stiffness correction coefficient
β	Stiffness correction coefficient
δ	Angle
μ	Ductility
ϕ	Curvature
ϕ_y	Yield curvature
σ	Standard deviation of fragility curves
θ_{max}	Maximum rotation
θ_L	Rotation in the longitudinal direction
θ_T	Rotation in the transverse direction
θ_y	Yield rotation

LIST OF ACRONYMS/ABBREVIATIONS

ACI	American Concrete Institute
EQ	Earthquake
FC	Fragility Curve
FDD	Frequency Domain Decomposition
FEM	Finite Element Model
MAC	Modal Assurance Criteria
PEER	Pacific Earthquake Engineering Research Center
PGA	Peak Ground Acceleration
SDC	Seismic Design Code
WN	White Noise

1. INTRODUCTION

1.1. Objective

Turkey is one of the earthquake prone countries; therefore, condition assessment of transportation network in a timely manner is critical both due to economic and public safety reasons. Post-event damage assessment in structures typically requires a detailed and time-consuming visual inspection and evaluation which may be insufficient and subjective. Lack of information about damage in critical structures such as bridges may disrupt emergency response. In contrast with visual inspection, structural health monitoring can revolutionize the inspection of structures, particularly for rapid, remote, automated, and objective post-earthquake damage assessment. By installing appropriate sensors at critical locations on a bridge, transmitting the sensor data through a communication network, and analyzing the data through a software platform, the location and severity of bridge damage caused by earthquakes can be automatically, remotely, and rapidly assessed. Therefore, the primary aim of this thesis can be defined as the implementation of structural health monitoring to highway bridges and condition assessment via vibration-based identification.

On the other hand, another way of condition assessment may be the analytical simulation of structures. However, this method also has different limitations as well as uncertainties. For instance, after an earthquake, the most crucial limitation will be the selection of input motion. Without a free-field monitoring system close to the structure it is impossible to obtain actual time history record which must be used in the analysis. Even though the input motion is well-known, due to the modeling uncertainties such as material properties and nonlinear behavior of the members, the severity of the damage would not be predicted precisely. Moreover, computer simulations are widely used to estimate remaining capacities of structures before making critical decisions. For instance, nonlinear time history analysis and pushover analysis are used to develop fragility curves and capacity curves, respectively. However, due to the modelling uncertainties discussed above, the accuracy of remaining capacities is also questionable.

Hence, another objective of the thesis is to investigate effects of modelling uncertainties on the condition assessment and seismic vulnerability estimation of reinforced concrete bridges.

1.2. Literature Review

1.2.1. Structural Health Monitoring

Doebling *et al.* (1996) presented a review of structural health monitoring methods and applications carried out before 1996. The aim of monitoring is to detect, localize, quantify and characterize damage indicated by changes in measured vibration response of structures. Within the improvement of monitoring methods, traditional techniques such as visual-based inspection and experimental methods could be changed or at least modified with general findings of monitoring systems. A sketch is showed involving a consecutive procedure such as identification, location and extent of damage, and remaining life assessment. Essential statements are utilized about the future of structural health monitoring. It has been addressed that automation, replacing engineering judgment and computer models, would be the final aim; and more attention on nonlinear modelling techniques would be paid. Once the dependence on starting data or finite element models is abstained, much broader success, as in other applications such as machinery, would be obtained. Furthermore, the ambiguity on location and number of sensors must be depleted, and sensitivity of records to modal characteristics must be revealed. Finally, efforts on real-life applications, such as structures and field tests under operating conditions is encouraged. Nevertheless, several researches have presented that structural health monitoring is a forward subject for the future of civil structure, and may substantially make contribution to the safe use of infrastructures.

Sohn *et al.* (2004) provided another review which covered the works finished between 1996 and 2001. The researchers approached health monitoring of structures as a statistical model diagnosis paradigm characterized by procedures of “operational Evaluation”, “data acquisition, fusion, cleansing”, “feature extraction and information condensation”, “statistical model development”. As aforementioned in the past

reviews, major challenges waiting monitoring of structures were determined. One of them refers to the state that neither data nor finite element model is available, thus a learning mode which is not supervised must be adopted. The other one was the ability to find damage, which is a local phenomenon, through the global acceleration response records of a structure. In addition to that, the ability to eliminate the effects of environmental and operational sources from the real damage of structural members was questioned. These challenges must be overcome to avoid false indications.

Carden and Fanning (2004) provided another study which reviews time and frequency domain techniques. It has been stated that there is still a huge variety of methods and disagreements regarding with a lot of different viewpoints of structural health monitoring. The range of algorithms, the sensitivity problems of modal parameter switches, "lackness" of field experiments, incompetence of remaining life evaluations still stand as the primary problems, that structural health monitoring society should be dealt with. A crucial remark has been made on contribution of numbers and locations of sensors. At the end, as long as number of sensors used in a structure is limited, a special or an optimal solution is questionable.

Brownjohn (2007) presented one of the most recent reviews that questions the aims of structural health monitoring, as well as former works finished. Regarding with the review, a classification is carried out based on structural types. Moreover, sensors used in monitoring applications on structures are considered in details. Finally, practical questions, recent abilities and new motivations are specified.

1.2.2. System Identification

Shinozuka and Ghanem (1995) presented the results from a research effort whose aim was a comprehensive treatment of system identification techniques in structural engineering applications. In the first paper, the mathematical backgrounds of different identification techniques were presented whereas the second part of the research involved models of buildings subjected to a number of different loading conditions in laboratory conditions. The suitability of the mathematical model and the validity of

the identification algorithm were analyzed via the measurements of the experiments. Moreover, results were presented that demonstrated importance of monitoring the motion at different floor levels. One of the main conclusions of the study was about the robustness and simplicity of the identification algorithms. The more sophisticated algorithms yielded better results on some of the measurements whereas failing to converge for the remaining ones. Also, these algorithms were quite sensitive to the initial guess regarding the unknown parameters. Finally, the most important suggestion of the paper was to emphasize the implementation of simple and reliable identification algorithms.

Farrar and James (1997) presented the cross-correlation function between two response measurements made on an ambiently excited structure. The advantage of this system identification method over standard procedures that identify resonant frequencies from peaks in the power spectrum and damping from the width of the power spectrum is the ability to identify closely spaced modes and their associated damping. However, the proposed method is subject to window-dependent resolution bias errors. In this study, random errors were minimized by averaging numerous measurements when estimating the cross-power spectra. In order to verify the proposed identification method, it was applied to an in-service highway bridge where traffic provided the vibration source. The modal parameters such as frequencies, mode shapes and modal damping obtained from the proposed method were compared with the results of the conventional system identification methods.

Beck and Katafygiotis (1998) tried to achieve quantitatively documented accuracy in model predictions, with a methodology incorporating a Bayesian statistical framework into model updating procedure. The methodology is complemented with a secondary study inspecting model identifiability for multi-degree of freedom linear structural systems, addressed by Katafygiotis and Beck (1998). The core of the study, developing a procedure to find alternative proper models, is completed with numerical examples. The conclusions stated the inapplicability of updating analytical models starting from single model, by questioning the uniqueness of this model, providing the presence of different proper models.

Lus *et al.* (1999) introduced an identification method based on earthquake excited acceleration response measurements. The methodology integrated Eigen-system Realization Algorithm, and Observer/Kalman Filter Identification to identify dynamic properties of structural systems with multi-degree of freedom. The validity of the proposed technique is tried to be presented with case studies of an eight storey structure, and Vincent-Thomas bridge excited during Whittier and Northridge Earthquakes. The performance of the proposed technique has been showed in despite of noise in the acceleration response measurements and inadequate accelerometer numbers.

1.2.3. Damage Detection

Huang *et al.* (2002) presented a procedure for identifying the dynamic characteristics of a building and diagnosing whether the building was damaged by earthquakes, using the back-propagation neural network approach. The diagnosis is based on the fact that damage to a structure induces non-linear structural responses to earthquakes and considerably changes both the modal parameters, directly estimated from the weighting matrices of the neural network, of an equivalent linear system and the output errors predicted by a neural network trained for the structure without any damage. The feasibility of the approach is demonstrated through processing the dynamic responses of a five-storey steel frame, subjected to different strengths of the Kobe earthquake, in the shaking table tests.

Perry and Koh (2007) presented a genetic algorithm based output only strategy for identifying structural parameters and damage from incomplete, noise-contaminated acceleration measurements. They proposed a strategy involving simultaneous evolution of structural parameters and input force. To document the verification of the methodology they carried out a numerical study and an experiment in laboratory. In the numerical study, the system they performed consists of three shear buildings connected by two link bridges. The response of the entire system is simulated using the first five seconds of the NS component of the 1940 El Centro earthquake. Using the proposed strategy, the central building and the coupling forces of the links are identified. In the experimental study, a 7-storey steel frame is constructed and tested in

the laboratory. Three damage magnitudes and three damage locations are used to examine the performance of the proposed strategy. For the experimental case, while the results are reasonably good for the large damage levels, the strategy is less successful in distinguishing the true damage and false damage in the small and some medium damage levels.

Gul and Catbas (2008) presented an output-only system identification method based on the use of complex mode indicator functions coupled with the random decrement method. Unscaled flexibility and the deflection profiles obtained from dynamic tests are used for the condition assessment purpose. The proposed method was validated via laboratory tests on a steel grid at undamaged and damaged states. Furthermore, identification method is used to obtain dynamic properties of a long-span bridge.

Zhang *et al.* (2011) proposed a frequency domain sub-structural identification method in this study. The strategy is formulated based on the steady-state dynamics of a free-free substructure. To make the divide-and-conquer philosophy applicable to arbitrary excitations, the exponential window method is embedded in F-sub formulation to enforce causality requirement for discrete Fourier transform. To document the verification of the methodology they carried out three numerical studies and an experimental study. The numerical studies were a 12-DOF system, a larger 50-DOF system, and a system of three connected buildings. For the first two systems, both stiffness identification and damage detection were carried out whereas only stiffness identification was conducted for the third system. To further validate the proposed F-sub method, an experimental study was done on a 7-level small-scale steel frame. The experimental study considered six degree scenarios. Damage was created by physical cut of selected column members. Five different random forces were used in each damage scenario. Dynamic test was carried out three times for each of these five forces. The results obtained from the experimental study showed that the proposed method successfully identifies not only single large damage but also small damage in the presence of multiple damages.

Belleri *et al.* (2013) presented the damage assessment of a three-story half-scale precast concrete building through structural identification. The structure was tested under earthquake-type loading on the NEES large high performance outdoor shake table at the University of California San Diego in 2008. Modal identification has been performed using the deterministic-stochastic subspace identification method based on the measured input-output data. The effective modal parameters of the structure show significant changes at the different damage states. In general, the natural frequencies decrease, and the damping ratios increase as the structure is exposed to larger base excitations. They pointed out that the identified damping ratios in this study represent the system equivalent viscous damping ratios and cannot be used as the viscous component in nonlinear finite element analyses because in nonlinear models, hysteretic damping is explicitly taken into account by the nonlinear material behavior. The analysis of the identified mode shapes allows finding the location of damage. The discontinuities in modal rotations and curvatures allowed localizing both visually detected damages in the third floor and an undetected damage in the second floor, providing a useful tool for precast floor damage detection.

Dackermann *et al.* (2014) presented a response-only structural health monitoring technique that utilizes cepstrum analysis and artificial neural networks for the identification of damage in civil engineering structures. The method begins by applying cepstrum-based operational modal analysis, which separates source and transmission path effects to determine the structure's frequency response function from response measurements only. The proposed method was verified on both experimental and numerical models of the two-story framed structure. Joint damage was simulated by changing the condition of individual joint elements of the structure from fixed to pinned. To consider real-life applications and to investigate the robustness of the method to noise, the ambient vibration responses obtained from the numerical model are polluted with different levels of white Gaussian noise. When the results obtained from both experimental and the numerical studies are evaluated, it was concluded as that whereas the proposed method showed great success in the detection of the damage of the structure, it exhibited sensitivity to the level of the noise of the ambient vibration measurements. For instance, when the results of two studies were compared to each

other, the results of the numerical study are generally poorer than the outcomes of the experimental study, due to noise contamination.

Limongelli *et al.* (2014) presented the interpolation damage detection technique for the case study of the UCLA factor building, a real instrumented multistory steel structure. The first step in the application of the technique is the characterization of the statistical variation of the interpolation error in the undamaged state of the building based on responses measured on the structure during a long period. The first step was conducted using responses measured on the structure during a number of small magnitude earthquakes. In the second step, to investigate the interpolation damage detection method to detect and localize damage, a calibrated numerical model of the structure was developed and used to simulate different damage scenarios. According to the results of the latter step, it was observed that the capability of the method to locate damage is influenced by the level of noise and by the severity of the damage. Medium and severe damages can be detected easily for medium to high level of noise. However, in order to detect small reductions of stiffness, high quality signals must be recorded on the structure.

Bandara *et al.* (2014) presented an artificial neural network-based damage detection method using frequency functions, which can effectively detect nonlinear damages for a given level of excitation. The main objective of the article was to present a feasible method for structural vibration-based health monitoring, which reduces the dimension of the initial frequency response function data and transforms it into new damage indices and employs artificial neural network method for detecting different levels of nonlinearity using recognized damage patterns from the proposed algorithm. The proposed method was applied for the three-story bookshelf structure at Los Alamos National Laboratory where damages were introduced as nonlinear damages. The presented approach was applied in two stages. In the first stage, all damage cases were used to train neural network whereas in the second stage, damaged data which had not been used in the training data set were also used to predict damages of the structure in the testing stage. According to the results obtained from both stages, it was observed that the damage detection performance of the first one was higher than the latter

stage. The reason of this consequence was explained as that in the first stage same damage patterns of the training data set were used to validate and test the network. Nevertheless, the results of the second stage were also sufficiently accurate for damage detection with a maximum error 2

1.2.4. Bridges

Enright and Frangopol (1998) presented the time-variant reliability of reinforced concrete highway girder bridges. In this study, both load and resistance were considered as time dependent variables that determine the reliability of bridges. According to results of the study, it was shown that the coefficient of variation (COV) of live load has a strong influence on the cumulative-time failure probability of bridge. The COV of the damage initiation time has very little effect on the cumulative-time failure probability of bridges beyond a specified service life. For bridge systems models in which girders are degrading at different rates, the series system can be reduced to a smaller number of girders, provided that the remaining strength of the girders in the reduced system is substantially less than the remaining strength of girders eliminated from the original system.

Sohn *et al.* (1998) examined a linear adaptive model to discriminate the changes of modal parameters due to temperature changes from those caused by structural damage or other environmental effects. Two vibration tests were conducted during the summer of 1996 and 1997. The first data set from 1996 test was used to train the adaptive filter. The filter uses spatial and temporal distributions to determine changes in the first and second mode frequencies. The system defines a confidence interval for future values of modal parameters in order to discriminate between variation caused by temperature changes and those indicative of structural change or other environmental effects. The comparison of the prediction intervals obtained from the first data set and the measured frequencies from the second test data reveals that the bridge experienced a statistically significant decrease in the first and second mode frequencies. The reasons of this significant change were designated as the severe rain prior to the second test and the insufficient drainage system. According to these conditions, the consistent decrease

of the frequencies was mainly caused by the increase of the bridge mass as the Alamosa Canyon Bridge absorbed significant amount of moisture, and the bridge retained much of the rainfall on its surface.

Teughels and De Roeck (2003) presented an iterative sensitivity based finite-element model updating method in which the discrepancies in both the eigen-frequencies and unscaled mode shape data obtained from ambient tests are minimized. In finite-element model updating, an optimization problem was set up in which the difference between the experimental and numerical modal data have to be minimized by adjusting the uncertain model properties. The experimental eigen-frequencies and mode shapes were used for the tuning. Also in the FEM updating, the trust region strategy was used as an additional measure to improve the robustness of the updating procedure. The proposed method was applied to a real civil engineering structure, namely the highway bridge Z24 in Switzerland. Its damage pattern was identified using the eigen-frequencies and unscaled mode shape data obtained from ambient vibrations. The damage was represented by a reduction in bending and torsion stiffness of the bridge girder. Also, for the undamaged state, the soil stiffness was updated in order to obtain the correlation for the transversal mode.

Brownjohn *et al.* (2003) presented the dynamic testing and modal analysis used to identify the vibration properties and the qualifications of the effectiveness of the upgrading through the subsequent modal updating. The program covered measurements to estimate the nature of the dynamic response followed by full-scale dynamic test to identify modal parameters before and upgrading.

Feng *et al.* (2004) presented a neural network-based system identification technique to establish and update a baseline finite element model of an instrumented highway bridge based on the modal parameters including modal frequencies and mode shapes of the bridges. For this purpose, two highway bridges were instrumented and extensive vibration data were collected and modal parameters were extracted using frequency domain decomposition and peak picking methods.

Akgül and Frangopol (2004) presented a probabilistic framework that can be used for forecasting the lifetime performance of existing pre-stressed concrete bridges. Only superstructure components were considered and other components of bridges were excluded. Random variables and deterministic parameters were individually identified for pre-stressed girder bridges. In order to perform the lifetime performance analysis using the developed limit state equations, a corrosion propagation model was derived for pre-stressed girders. Using the developed limit state equations, the reliability indices were computed for the components of selected bridges in Colorado bridge network.

Brownjohn *et al.* (2004) presented the experience obtained by the structural health monitoring of different bridges for different aims. According to experience of four bridge monitoring systems, different recommendations were made for future bridge health monitoring projects. Clarity of Purpose was the first recommendation. This part was constructed on the major differences between the relatively basic requirements of bridge managers and the ambitions of system designers who were thought as academics in the paper. As the second recommendation, Novel Sensors and Embedded Systems were crucial for future monitoring. They pointed out the importance of the multidisciplinary approach for the improvement of new systems. Another important factor in the SHM was explained as the communication. The revolutions in the technology such as GPRS and 3G would help to make cabling redundant thereby removing probably the greatest headache in instrumentation.

Phares *et al.* (2004) presented the result of the study related to the accuracy and reliability of routine inspection documentation. The complete study consisted of 10 field inspection tasks including seven routine tasks. Six of the routine inspections were individual inspections whereas the seventh task was to complete the inspection as a team. Based on the inspections completed in the investigation, several observations and conclusions were obtained. Routine inspection documentation of structural conditions showed significant variability. Most inspectors used photographs to document the overall condition of a structure where as they must be used to show the condition of structural elements. Finally, there was significant variability in the condition state assignment to commonly recognized elements. According to the results of this study,

it can be concluded as that the result of a visual inspection is dependent to inspector. In other words, a visual inspection method is not an objective way to assess structural conditions.

Xia and Brownjohn (2004) presented a method using a systematically validated finite-element model for the quantitative condition assessment of a damaged reinforced concrete bridge deck structure, including damage location and extent, residual stiffness evaluation, and load-carrying capacity assessment. The first step was pre-validating the FE model for the undamaged state. For this purpose, the stiffness of the boundary supports, the Young's modulus, and the mass density of the concrete were selected as the updating parameters. In the second step, post-validating the FE model for damaged structure was done to identify the damage and assess the structural condition. The moment of inertia of the beam and the cross section area were taken as uncertain parameters to update the model. Finally, authors used the relationship between the moment of inertia and the steel ratio in order to determine the ultimate moment and load-carrying capacity of the damaged structure.

Mackie and Stojadinovic (2005) presented a method for evaluating the functionality of a typical highway bridge after an earthquake in a quantitative way. In order to make a quantitative estimation, three limit states, which are repair cost, traffic function, and collapse prevention, are determined. The PEER framework was utilized to cast these limit states in terms of damage and decision fragility curves.

Guan and Karbhari (2006) presented the results of an investigation into the development of a web-based monitoring system installed on an FRP composite bridge. The response of the bridge was characterized through various sensors whereas a camera system was used to correlate traffic conditions with other sensor measurements. In this investigation, the time domain decomposition was used to extract modal parameters from sets of measured dynamic response of a given structure.

Liu *et al.* (2008) presented the dynamic experiments and the experimental validation of two approaches for the prediction of the bridge response due to the passage

of the high-speed trains. The Sesia viaduct, with a total length of 322m, was used in the presented study.

Bayraktar *et al.* (2009) presented the dynamic characteristics of the Kömürhan Bridge located on the Elazığ-Malatya Highway in Turkey. The modal parameters such as natural frequencies, mode shapes and damping ratios of the structure were obtained from both an analytical model of the bridge and ambient vibration survey and compared with each other. From the result of the comparison, it was seen that there was a good harmony but little difference between frequencies. The reason for this difference was mentioned as the structural geometry, material properties and boundary conditions used in the modeling of the bridge.

Chen *et al.* (2009) proposed a stochastic model of traffic excitation on bridges. The presented model assumes that the arrival of vehicles traversing a bridge follows a Poisson process and that the contact force of the vehicle on the bridge can be converted to equivalent dynamic loads at the nodes of the beam elements. The validation of the procedure was conducted via a highway bridge monitored with acceleration sensors for vibration measurements and video-based monitoring system for traffic loads.

Soyoz and Feng (2009) presented the structural identification results of a highway bridge over a five-year period. Based on the vibration data, the bridge structural parameters including mass and stiffness, as well as modal parameters, were identified. It was observed that during the five-year period, fundamental frequency and superstructure stiffness of the bridge were decreased. Moreover, a fluctuation, due to environmental effects, in both frequency and stiffness were investigated over the same period.

Altunisik *et al.* (2011) presented the dynamic-based assessment of a restored historic arch bridge. The study covered 3D finite element modeling, Operational Modal Analysis and finite element model updating. In order to obtain the dynamic characteristics of the bridge, an ambient vibration survey was carried out. From experimental measurements, natural frequencies, mode shapes and damping ratios of the structure

were obtained. Afterwards, finite element model of the bridge was constructed in order to find modal parameters of the structure in an analytical way and to compare them with the measured results. Since there is a difference between the measured and estimated parameters of the structure, a model updating procedure was carried out in order to obtain a more representative finite element model of the bridge.

Gomez *et al.* (2011) presented the findings of the analyses of eight years of monitored data from the West Street on Ramp which is a curved post-tensioned reinforced concrete box girder bridge in California. The motivation of this study was to demonstrate the practical use of monitored data for long-term structural condition assessment and to examine the potential of vehicle mounted sensors in determining bridge frequencies in the absence of sensors mounted on a bridge.

Mosquera *et al.* (2011) presented a vibration-based damage detection technique that uses the difference between the actual measurement of the structural response and the predicted one by an identified linear state-space model. In the study ERA/OKID is applied to identify the first-order state-space model of the Meloland Road Overpass, using low amplitude earthquake records which do not lead to the presence of any nonlinear behavior in the structure. The same algorithm was used to detect the damage on the structure for high amplitude excitations. Since the ERA/OKID is a linear method, the difference between the predicted acceleration response by the algorithm and the measured response will be used as a first criterion to determine whether the structure has suffered damage or not.

Altunisik *et al.* (2013) presented the analytical and experimental modal analyses of a scaled bridge model. The structure presented in this study was a bridge model constructed in laboratory conditions. In order to obtain the dynamic characteristics of the bridge model, 3D finite element model of the structure was constructed using SAP2000. Afterwards, in order to compare the analytical results obtained in the previous step with the real modal parameters of the bridge, ambient and forced vibration tests were conducted.

Westgate *et al.* (2013) presented a site investigation on the performance of Tamar Suspension Bridge during the passage of a heavily laden vehicle, which provided an opportunity to observe changes in response to a travelling concentrated mass, with an unusual ration of vehicle and bridge weights. The study was limited to effects of the additional mass along with changes in the bridge configuration and tensions of main cables and additional stays. It was observed that the frequency of vertical modes decreased as the additional mass of the trailer moved towards the part of the structure with largest modal ordinate. The frequencies of lateral modes related more to changes in the cable tensions, and increased as a result of tension stiffening more than they reduced due to added mass.

Gomez *et al.* (2013) summarized their findings from the application of different identification methods to the acceleration records measured from a bridge under six earthquake events. Targeted dynamic properties are natural frequencies and damping ratios. According to comparison of identification results, difference of the fundamental frequencies obtained using different methods was nominal whereas for the higher frequencies, it increased. However, for the damping, the difference reached significant levels. A general conclusion from the study was that larger earthquake intensities result in reduction of frequencies and higher damping ratios. Moreover, sensitivity analysis using a simple finite element model indicated that, due to the changes in support conditions, soil softening might be the primary reason of the variation in frequencies.

Reynders *et al.* (2014) presented an improved technique based on kernel principal component analysis in order to eliminate environmental and operational influences on structural health monitoring and damage detection. The proposed technique has three stages: the first stage is data reduction by identification of damage-sensitive features such as modal characteristics in short time period, the second one is the identification of a nonlinear environmental model using the damage-sensitive features from the previous stage as outputs and the final stage is monitoring the prediction error of the global model.

1.2.5. Reliability Estimation

Park *et al.* (1985) introduced a method to estimate structural damage of reinforced concrete structures under earthquake events. In this context, a relationship is developed between structural damage and earthquake intensity. Moreover, such algorithm contained calibration according to damages of reinforced concrete structures due to previous earthquakes. Eventually, a quantitative damage estimation expression as a function of ground motion is presented. Such evaluation contained probabilistic terms, which provided one of the milestones in reliability-based aseismic design.

Singhal and Kiremidjian (1998) proposed a Bayesian statistical analysis technique to update the relationship between structural damage and earthquake intensity. Such analysis is carried out in the form of analytical fragility curve. Moreover, analytical fragility curves are integrated with structural damage data from previous earthquakes. In this scheme, analytical content stood for prior distribution, whereas data on structural damage established likelihood function with the interference of Park and Ang damage index as a random variable. Consequently, updating is performed to achieve posterior distribution. Such updating strategy enabled to improve accuracy of fragility curves, which are based on periodic calibration of reliabilities with the appearance of recently available damage data.

Shinozuka *et al.* (2000) presented fragility curves of bridges with two different approaches such as the one obtained from time history analysis, and the another one based on capacity spectrum method. Hence, fragility curves were compared with each other. It was revealed that reliabilities obtained from two methods lost the correlation as damage level rose from minor to major state. Such statement was presented as a result of increasing nonlinear effects with the increasing damage level. Nevertheless, proper agreement was obtained between fragility curves of two methods for high damage states. For low damage states, such agreement had proven to be excellent.

Shinozuka *et al.* (2000) carried out a study which combined analytical and empirical fragility curves in a statistical scheme. In this study, analytical fragility curves

are developed according to nonlinear dynamic analysis. Furthermore, extensive data collected from 1995 Kobe Earthquake is utilized for revision of analytical fragility curves. As a conclusion, ability to obtain integrated or composite curves is achieved, which leads to make widely representative fragility estimates, rather than case specific estimates.

Banerjee and Shinozuka (2008) presented performance evaluation of bridges in a probabilistic manner. Quantitative measures of seismic "damagability" information is supplied by a combined procedure of analytical, experimental and empirical approaches. Analytical study is performed with the incorporation of empirical information to produce a mechanistic model. Experimental data, with regards to physical damage descriptions, is obtained from a large-scale shaking table test. Finally, combination of analytical, empirical, and experimental results is proven to be coherent. Hence, threshold limits for damage description in bridge columns is quantified and verified.

Frangopol *et al.* (2008) proposed a combined procedure of structural health monitoring and reliability estimation. A practically applicable method has been stated to make use of such combined procedure. Moreover, probabilistic prediction models would be developed according to health monitoring findings. Statements are provided with exemplary works, which are supported with an optimization procedure for operational cost of structural health monitoring applications.

Catbas *et al.* (2008) introduced a reliability estimation method with the inclusion of long-term monitoring measurements. Structural health monitoring of the longest span truss bridge in the US subjected that reliability excitations are significantly affected by environmental and operational changes. Findings of the study have shown the necessity of health monitoring systems for eliminating or reducing uncertainties related with load and temperature to obtain adequate reliability estimations.

Ghosn *et al.* (2016) presented a study that reviews the reliability-based performance criteria for designing new structures and assessing the existing ones. Since

reliability is one of the most important tools used to evaluate the future performance of structures, different methods have been studied and proposed by researchers. In this paper, both member-based and system-based methods were investigated. The most critical conclusion of the paper is that despite the similarities, available reliability methods are based on varied performance indicators. Additionally, for the application, these methods have some limitations related with monitoring and modelling of deterioration of structural members.

1.2.6. Nonlinear Modelling

Pankaj and Lin (2005) showed the influence of material modeling on the seismic response of reinforced concrete frames. They summarized that there is a significant difference in the structural response under response history analysis due to two different material models.

Inel and Ozmen (2006) presented their analytical study on the possible difference in the result of pushover analysis due to default and user-defined nonlinear properties. Their conclusion is that for the existing buildings constructed before the modern codes, the user-defined hinge model can represent the nonlinear behavior better than the default-hinge can do.

Goulet *et al.* (2007) presented a study on the evaluation of the seismic performance of a code-conforming reinforced concrete frame building. They concluded that collapse probability is highly sensitive to structural modeling uncertainties and realistic estimates of plastic rotation capacity are essential for accurate collapse predictions. They also said that the fiber model is less numerically stable during the pushover analysis whereas the plastic hinge model is capable of capturing strain-softening behavior that the fiber model cannot.

Bardakis and Dritsos (2007) presented the influence of different assumptions of the American and European codes. Due to the difference in the effective yield points of two codes, at the high-level excitation structural behavior differs significantly.

Shattarat *et al.* (2008) presented their study which compares the seismic response of a highway bridge using different software programs. They summarized that due to the difference in the plastic hinge models of different software programs, pushover curves obtained by them differ between each other significantly.

Lepage *et al.* (2010) summarized their findings about the optimal combination of hysteresis-modelling parameters for use in nonlinear analysis.

Yazgan and Dazio (2011 I and II) introduced their studies on the accuracy and sensitivity of the simulated maximum and residual displacements of reinforced concrete structures. They presented that different nonlinear modeling approaches can result in different accuracies in simulating non-linear response of structures.

Celarec and Dolsek (2013) presented the impact of modeling uncertainties on the seismic performance of reinforced concrete frame buildings. They concluded that the rotational capacity of the plastic hinges in the structural has the greatest influence on the seismic response parameters.

Ergun and Demir (2014) studied the effect of hysteretic models on displacement demands of reinforced concrete structures having various irregularities. Their conclusion is that the hysteretic models have a significant effect on displacement demands of reinforced concrete structures.

Eslami and Ronagh (2014) presented the effect of plastic hinge definition on the pushover analysis of reinforced concrete buildings. They compared the results obtained using FEMA based and user-defined hinge models. Their findings showed that models based on the FEMA hinges did not predict the displacement ductility of the RC frames adequately.

1.3. Thesis Outline

In the first chapter, a literature review regarding structural health monitoring, system identification and reliability estimation is presented. Furthermore, the scope and the objectives of work has been denoted.

In Chapter 2, instrumentation and monitoring of a real bridge in Istanbul are explained and examples of vibration measurements and database of modal parameters measured during long-term monitoring are presented.

Chapter 3 starts with the development of finite element model of the structure. In this part, effects of simplifications on the dynamic characteristic of the bridge are investigated. Afterwards, the improvement of finite element model using empirical equations for soil-structure interaction of abutments and footings is presented. This chapter is completed with identification of structural parameters via modal analysis of measurements and finite element modal updating.

In Chapter 4, validation of the system identification method used in the previous chapter is presented. For this purpose, measurements of a four-span three-bent reinforced concrete bridge model tested at University of Nevada-Reno are used. Identified structural parameters at different damage states are compared with calculated ones according to curvature measurements and results clearly indicates that the proposed system identification method is capable of condition assessment of highway bridges. Moreover, in this chapter, effects of modelling uncertainties regarding with nonlinearity of structural elements on condition assessment and seismic vulnerability estimation are presented. For the condition assessment purpose, earthquake excitations used in the experiment are used in the nonlinear time history analyses of the bridge whereas, in the seismic vulnerability estimation part fragility curves, as a function of peak ground acceleration, are developed.

In the last chapter, conclusions are presented and the future work suggestions have been made.

2. DESCRIPTION OF BRIDGE, MONITORING SYSTEM AND VIBRATION MEASUREMENTS

2.1. Etiler Bridge and Monitoring System

This section explains the tested bridge and the monitoring system used to identify its dynamic characteristics. The investigated structure is a four-span, reinforced concrete, highway bridge. Total length of the bridge is 84m and the height of the columns is 6.5m. Figure 2.1 presents the location of the bridge and Figure 2.2 shows the structure.



Figure 2.1. Location of the bridge.



Figure 2.2. Etiler bridge.

2.1.1. Long-Term Monitoring System

Acceleration sensors are used to obtain transverse, longitudinal and vertical natural frequencies and mode shapes of the bridge. Eight accelerometers are located on the superstructure and columns in order to obtain its dynamic characteristics whereas three sensors are located on the ground level to trigger the data acquisition system under an earthquake event.

Since the environmental conditions have crucial effects on the dynamic features of bridges, a temperature sensor is started to be used in addition to eleven accelerometers recently. Figure 2.3. presents the sensor layout and Figure 2.4 to 2.6 show sensors located on the structure.

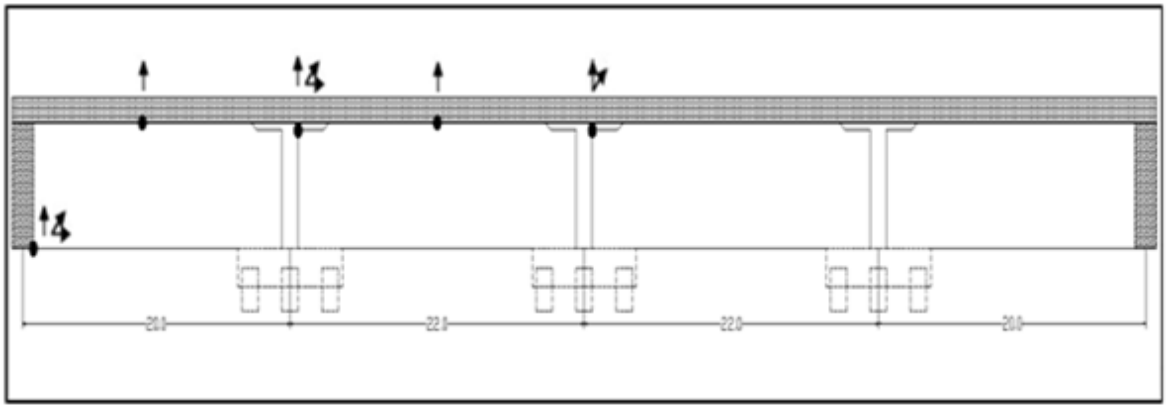

Figure 2.3. Sensor layout of the bridge.



Figure 2.4. Sensors located at the ground level.



Figure 2.5. Sensors located on the first column.



Figure 2.6. Sensors located on the second column.

2.1.2. Short-Term Monitoring System

The third and fourth spans and third column of the bridge could not be instrumented due to the safety reasons about cable-carrying system and high vehicles passing under the bridge. Therefore, another accelerometer was used at these locations in order to obtain the transverse and vertical mode shapes of the structure. Figure 2.7 and 2.8 show the sensor used during the short-term monitoring. Synchronization problems related with the short-term monitoring was eliminated using the long-term monitoring system during this stage.



Figure 2.7. Short-term monitoring of the third column.



Figure 2.8. Short-term monitoring of the third span.

2.2. Vibration Measurements and Long-Term Database

The primary aim of the long-term monitoring of a structure is to detect any structural changes at the earliest possible stage. For this purpose, a database must be developed carefully to store vibration measurements and modal values of the structure. The monitoring system used on Etiler bridge automatically measures vibrations due to traffic loads every day for a period of an hour. Afterwards, these measurements are collected and their modal analyses are conducted periodically in order to observe whether there is a change in modal frequencies and mode shapes or not. Figure 2.9 and 2.10 presents examples of vibration measurements in transverse and vertical directions. The results of the long-term monitoring of modal frequencies are presented in Figure 2.11 and 2.12 for transverse and vertical directions. Details about the identification method are presented in the next chapter. As it can be seen from these figures, the modal values did not change in the period of almost two years. The reason of this situation may be that the completion of the construction of Etiler bridge was very close to the beginning of the project and hence bridge is structurally very young. Therefore, it may be claimed that if the monitoring would continue in the coming years, changes in modal frequencies due to aging will be measured. Moreover, it would give an interesting opportunity to investigate the rate of deterioration of the bridge in different periods of its life.

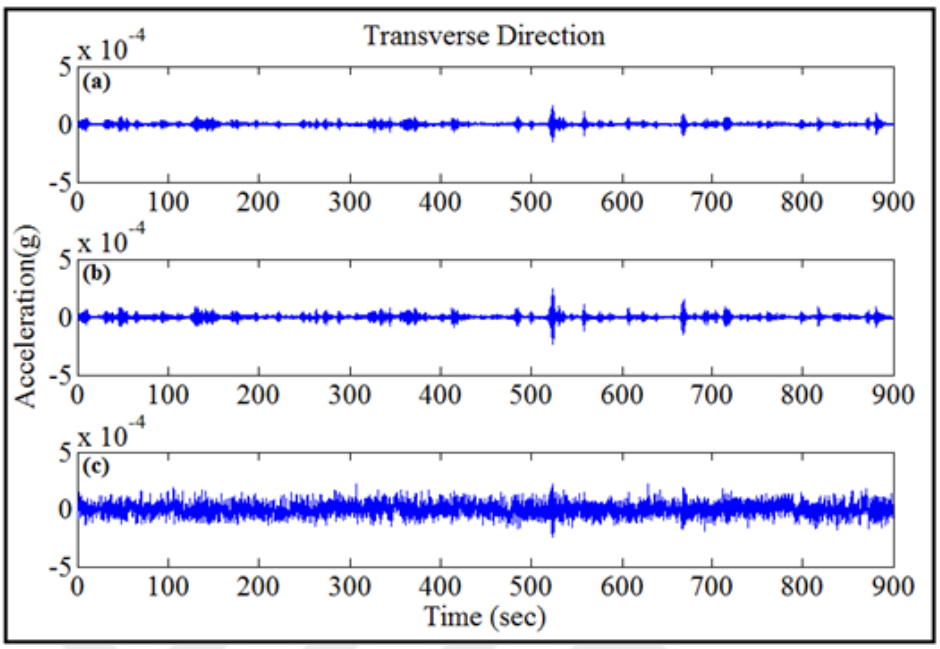

Figure 2.9. Vibration measurements in the transverse direction: (a) to (c) show Bent-1 to Bent-3.

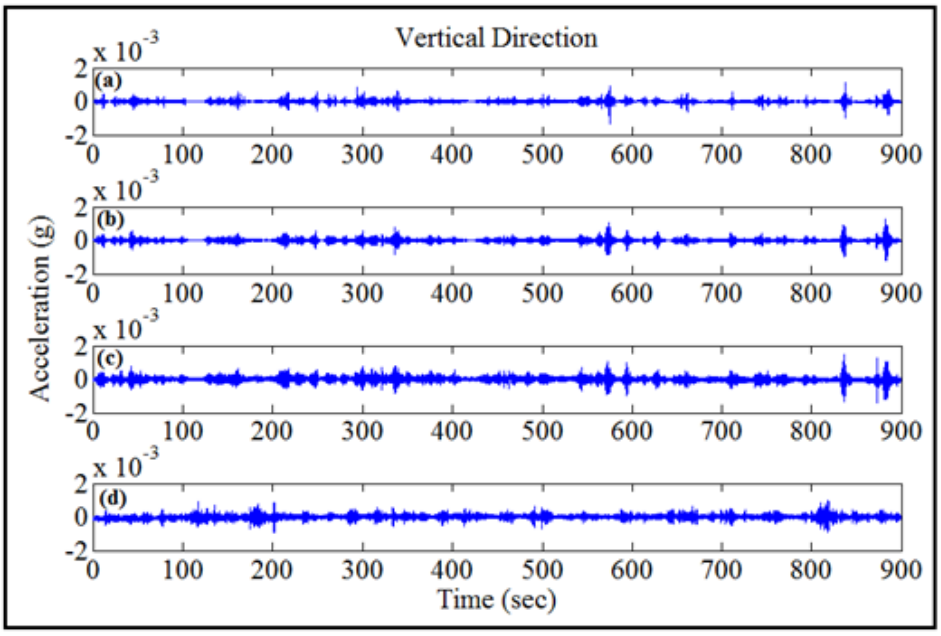

Figure 2.10. Vibration measurements in the vertical direction: (a) to (d) show Span-1 to Span-4.

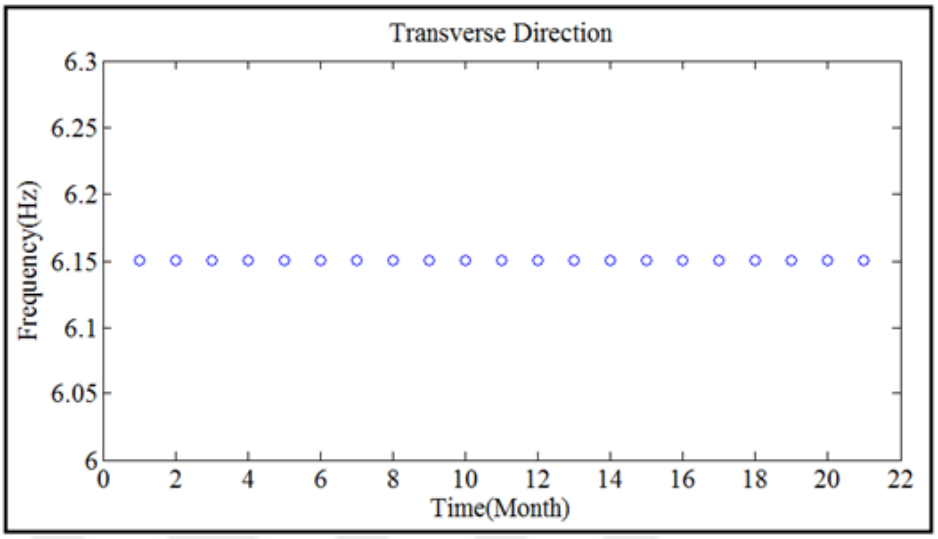

Figure 2.11. First modal frequency in the transverse direction.

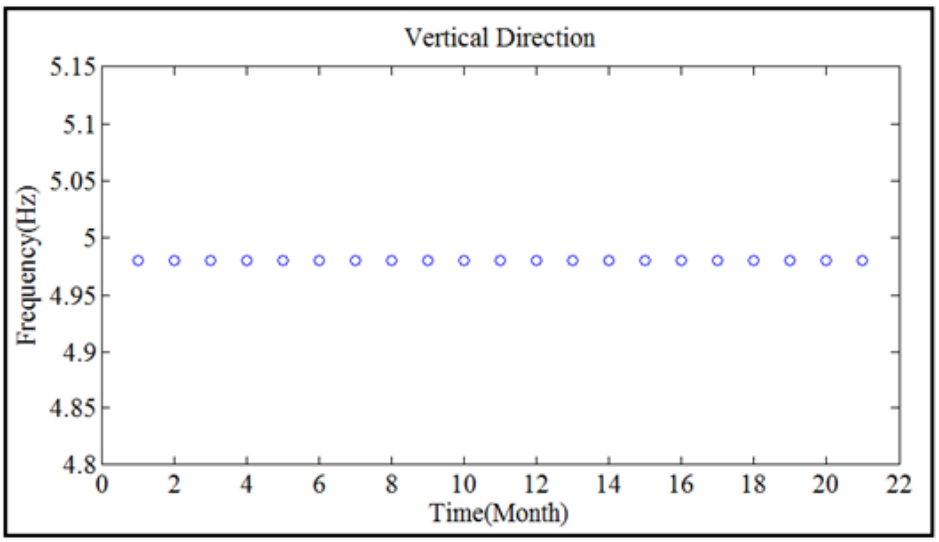

Figure 2.12. First modal frequency in the vertical direction.

3. SYSTEM IDENTIFICATION AND FINITE ELEMENT MODEL UPDATING OF THE BRIDGE

3.1. Design Drawings and Initial Finite Element Model

This section explains the finite element modelling procedure of the structure. Discussions involved in this section are essential to demonstrate the validity of modelling approaches. Finite element modelling and modal analyses are carried out with the structural analysis program, SAP2000.

3.1.1. Simplified Model of the Bridge

The modelling of the bridge was started with constructing a simplified finite element model. Herein the simplified is used for modelling of abutment locations. The investigation of the effects of modelling approaches of abutments on dynamic characteristics of the structure will be presented in the next section. Therefore, the initial finite element model of the bridge is generated using design drawings and material properties of only deck and columns. According to design documents, C30 concrete was used for the deck and C25 concrete was used for columns. Figure 3.1. to 3.4. present design drawings of the bridge. Modulus of elasticity of reinforced concrete is expressed by many different design codes and regulations in terms of 28-day strength of concrete. In these study, the Equation 3.1 provided by American Concrete Institute(ACI) Code (2008) is used.

$$E_{cj} = 4700\sqrt{f_{cj}} \tag{3.1}$$

where

E_{cj} : the modulus of elasticity

f_{cj} : the compressive strength

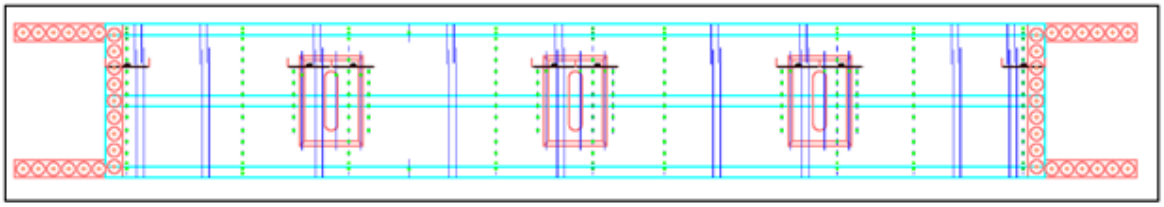

Figure 3.1. Top view of the bridge.

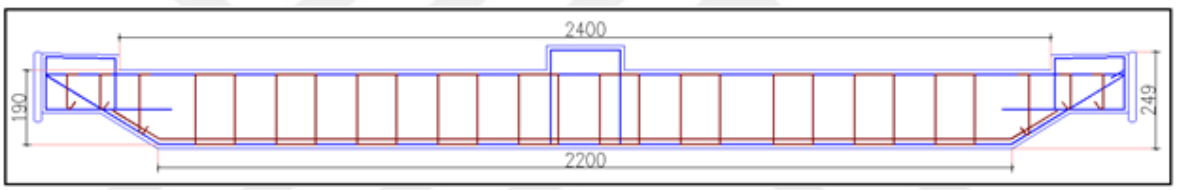

Figure 3.2. Elevation view of the deck (unit is cm).

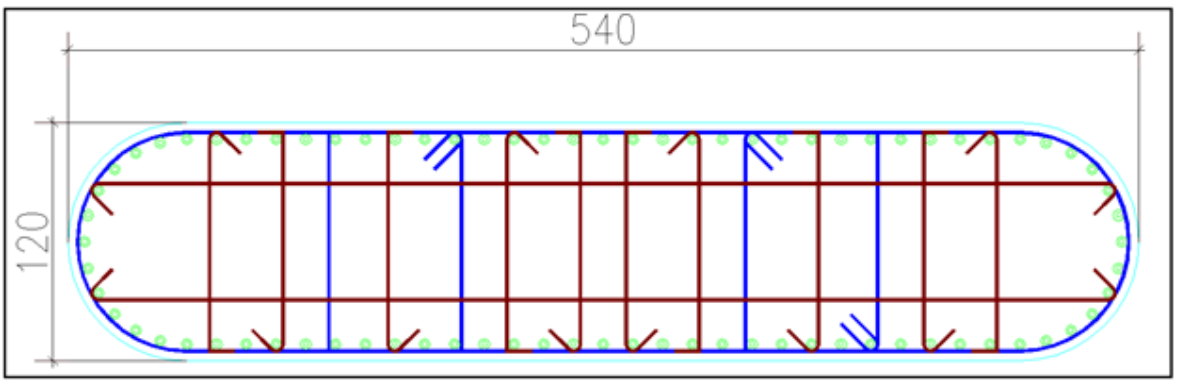

Figure 3.3. Top view of the columns (unit is cm).

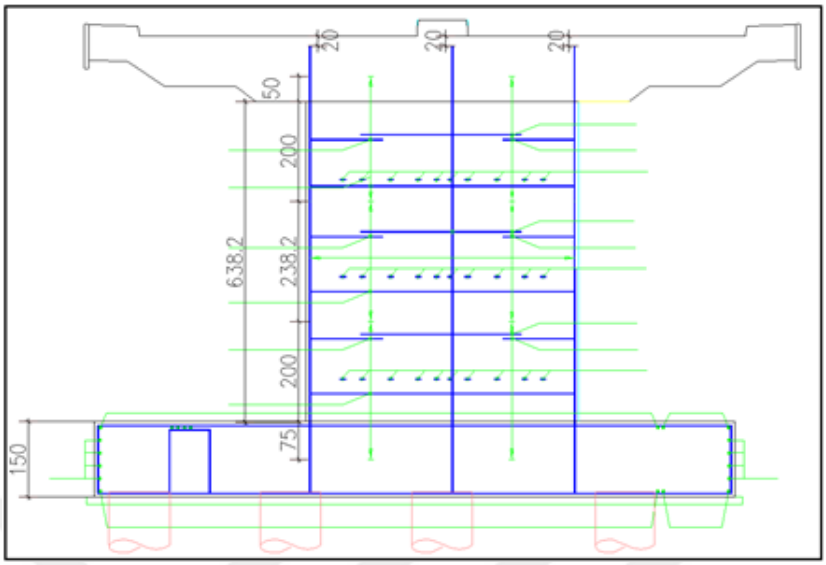

Figure 3.4. Elevation view of the columns (unit is cm).

Figure 3.5. shows the simplified finite element model of the bridge. Structural elements, deck and columns, were modelled using frame elements and dimensions were obtained from above design drawings. Two extreme cases of abutment modelling were taken into account in order to observe the effects of simplification on dynamic characteristics of the bridge. The first one is fixed support and the second case is free support. In latter case, only the vertical movement of the structure is fixed whereas the former model does not allow any movements.

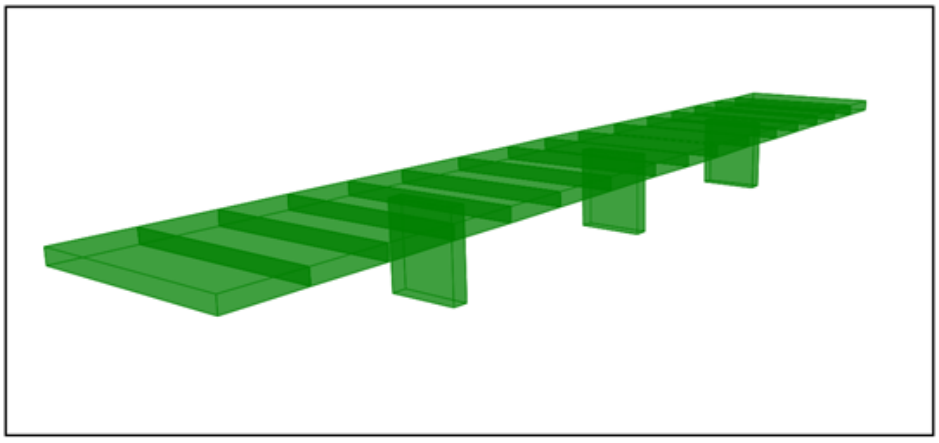

Figure 3.5. The simplified finite element model of the bridge.

Table 3.1 presents the difference in modal frequencies obtained from finite element models using two simplifications. The differences are 73%, 37% and 18% for the first, the second and the third frequencies in the transverse direction respectively. Structural responses under earthquake excitations will differ significantly due to these difference in the dynamic characteristics of the bridge. Therefore, the detailed modelling of abutments is required to obtain an accurate finite element model and realistic simulations.

Table 3.1. Comparison of modal frequencies in the transverse direction obtained by two models.

	Fixed Support	Free Support	Difference %
Mode 1	11.04 Hz	2.94 Hz	73.4
Mode 2	17.05 Hz	10.72 Hz	37.1
Mode 3	26.18 Hz	21.22 Hz	18.9

3.1.2. Modelling of the Abutments

The improvement of the simplified model is started with modelling the abutments that support the deck. The abutments of Etiler bridge is constructed as diaphragm systems. Figure 3.6 show the side view of abutments. The essential structural difference between seat and diaphragm abutments is that the first abutment type permits superstructure movement independent of the abutment while the second type does not. The short seat abutment is an independent structural component of the bridge and can generally be designed to accommodate all the imposed forces whereas the diaphragm abutment engages the adjacent backfill immediately which is very effective in absorbing energy during an earthquake. The longitudinal resistance for seismic analysis of a diaphragm abutment should be based on mobilizing the backfill equal to the depth of the superstructure plus the shear capacity of the abutment diaphragm. The transverse resistance for seismic analysis for a diaphragm abutment should be based on the ultimate shear capacity of one wing wall and all piles. The limiting force for transverse

keys for diaphragm abutments on footings is the ultimate shear capacity of the piles. This force represents the maximum force which can be expected to be transmitted through the keys. The top view of abutments is presented in Figure 3.7.

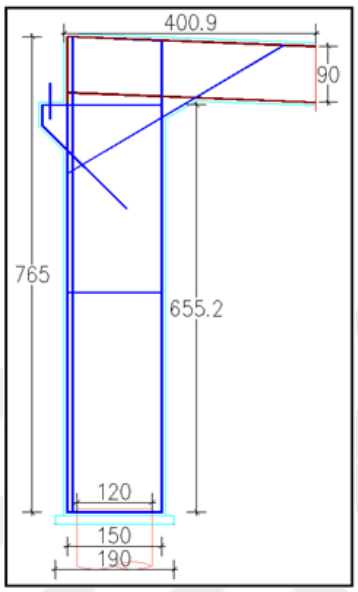

Figure 3.6. Side view of abutments (unit is cm).

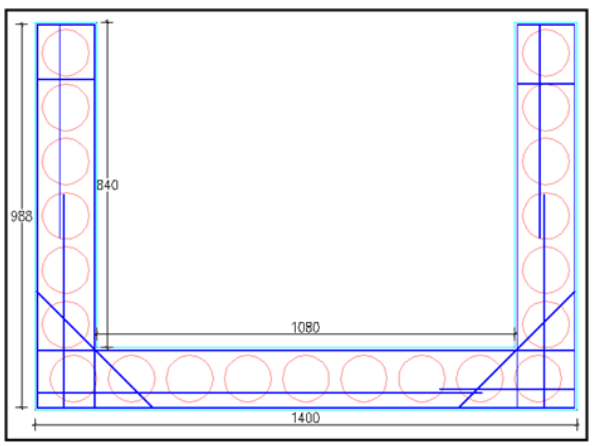

Figure 3.7. Top view of abutments (unit is cm).

The wall connected to the deck of the bridge is modelled with both frame and shell elements in order to investigate effects of two modelling approaches. On the other hand, stiffness contributions of the diaphragm system in the longitudinal and transverse directions are modelled using spring elements. The stiffness values are calculated using

Equations 3.2 to 3.5 according to Caltrans SDC 1.7 and Aviram et.al. (2008). Figure 3.8 and 3.9 show the finite element model of the bridge constructed using frame and shell elements in the abutment modelling.Tables 3.2 and 3.3 present the comparison of modal frequencies obtained using two models in the transverse and longitudinal directions respectively. Even though the difference in the first modal frequencies of transverse direction is relatively small, differences of the second and third modes of the same direction are around 20-30%. Moreover, in the longitudinal direction, values of the first mode differ 22% when the second mode disappears in the model with shell elements. Therefore, the model with frame elements was chosen to finalize the improvements of finite element model.

$$K_l = K_i * w * \frac{h}{1.7m} \tag{3.2}$$

$$K_t = K_l * C_L * C_W \tag{3.3}$$

$$P_{dia} = A_e * (239kPa) * \frac{h}{1.7} \tag{3.4}$$

$$A_e = h * w \tag{3.5}$$

where

K_l : Longitudinal stiffness of the diaphragm

K_t : Initial stiffness of the backfill

K_t : Transverse stiffness of the diaphragm

w : Width of the diaphragm wall

h : Height of the diaphragm wall

C_L : Effective coefficient of diaphragm wall

C_W : Contribution coefficient

A_e : Effective area of the diaphragm wall

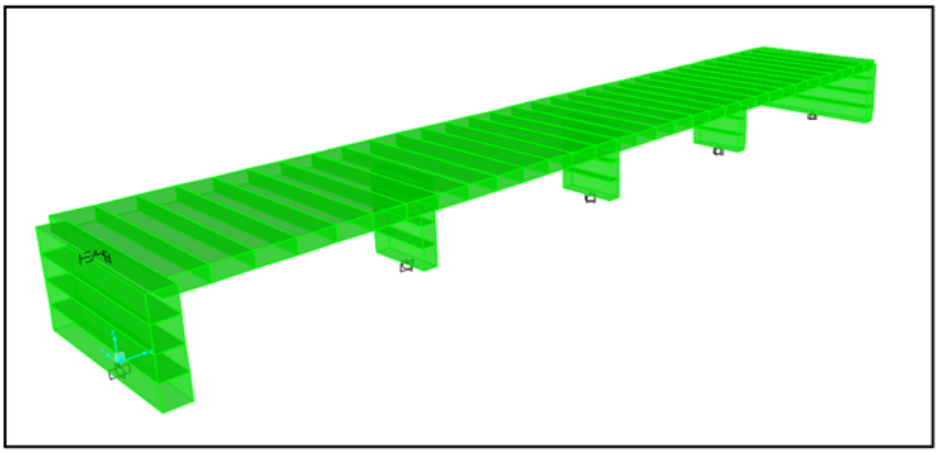

Figure 3.8. Finite element model with abutments using frame elements.

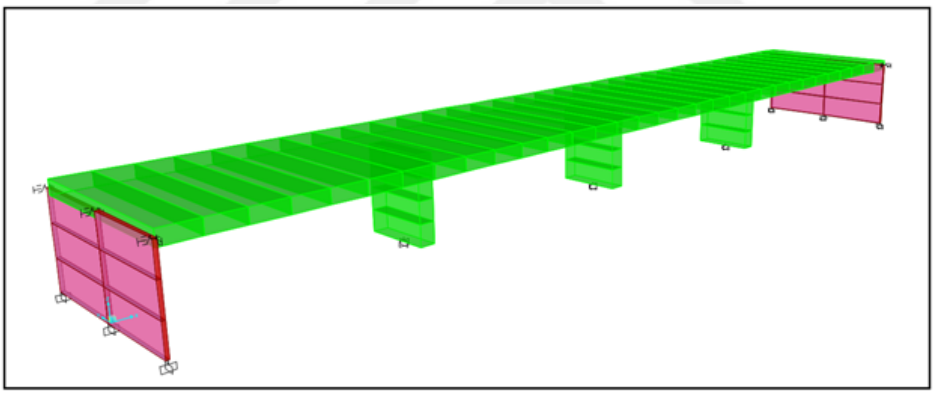

Figure 3.9. Finite element model with abutments using shell elements.

Table 3.2. Comparison of modal frequencies in the transverse direction.

	Frame elements	Shell elements	Difference %
Mode 1	9.79 Hz	9.50 Hz	2.96
Mode 2	13.98 Hz	11.37 Hz	18.67
Mode 3	21.80 Hz	15.15 Hz	30.50

Table 3.3. Comparison of modal frequencies in the longitudinal direction.

	Frame elements	Shell elements	Difference %
Mode 1	6.78 Hz	5.28 Hz	22.12
Mode 2	7.53 Hz	-	-

3.1.3. Modelling of Footings

Improvements of the finite element model was finalized with modelling of footings. Since the displacements at the bottom points of piers and diaphragm walls are insignificant, they are restricted in the model. Rotational stiffness values are calculated according to Equation 4.6 which is obtained from Priestley et.al (1996) and Aviram et.al (2008).

$$K_r = \frac{1}{12} * B_F * D_F * k_s \tag{3.6}$$

where

K_r : Rotation Stiffness Value

B_F : Width of the Footing

D_F : Depth of the Footing

k_s : Coefficient of Soil Reaction

Table 3.4. Comparison of modal frequencies in the vertical direction.

	Fixed Model	Free Model	Final Model
Mode 1	11.04 Hz	2.94 Hz	6.73 Hz
Mode 2	17.05 Hz	10.72 Hz	9.86 Hz
Mode 3	26.18 Hz	21.22 Hz	13.91 Hz

Figure 3.10 shows the final model developed according to design drawings and references and frequencies in the transverse direction obtained by different models are presented in Table 3.4.

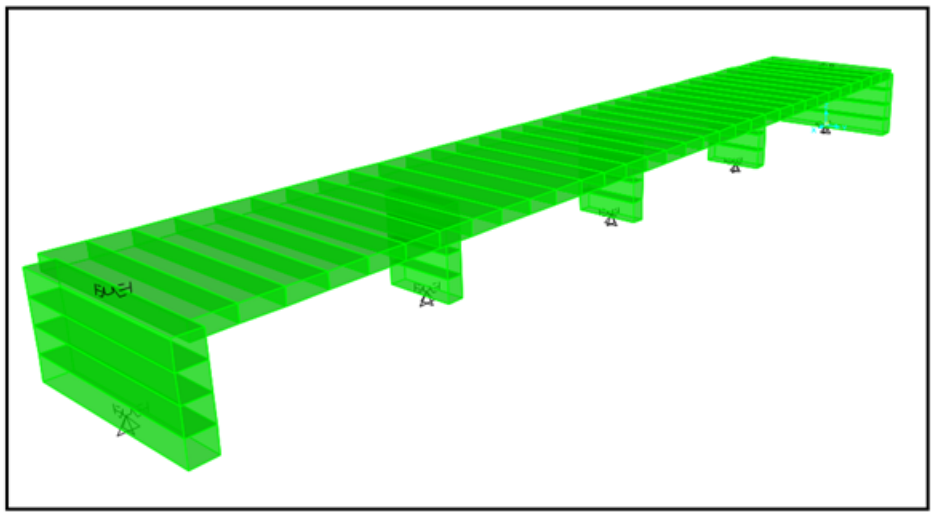

Figure 3.10. Finite element model of the bridge developed according to design drawings.

3.2. System Identification

System identification methods could be basically divided into two groups such as frequency domain methods and time domain methods. In this study, identification is carried out in frequency domain using vibration measurements. The identification strategy is based on the fact that the system is linear time-invariant, which means that structure experiences no damage-change throughout the observation.

Structural identification in the frequency domain has two steps. The first step is the identification of the modal values using the acceleration measurements of the bridge. The second step is the minimization of the error between the modal values obtained from the FEM and the measurements, which is called as model updating or model calibration.

An output-only method, the Frequency Domain Decomposition (FDD) method (e.g., Otte *et al.*, 1990; Brinker *et al.*, 2001) was used to extract modal parameters from the vibration measurements without requiring information for input. For this purpose, an in house Matlab code was used instead of buying a commercial software. The FDD method is capable of identifying closely coupled modes, thus obtaining better estimates compared to other modal identification methods (Otte *et al.*, 1990). In this method, spectral density matrix $S_{YY}(w)$ of the response vector Y(t)is decomposed by singular value decomposition, as illustrated in the equation

$$S_{YY}(w) = U(w) \sum (w) U^H(w) \tag{3.7}$$

where

$\sum(w)$: Diagonal matrix of the singular values

$U(w)$: unitary matrix of the singular vectors

the superscript H denotes the complex conjugate and transpose

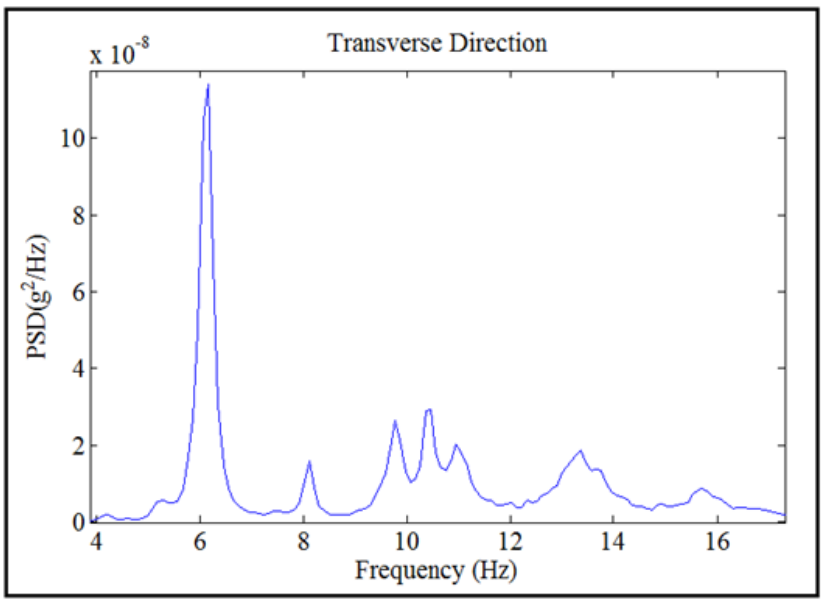

Figure 3.11. Power Spectral Density of the Bridge in the Transverse Direction.

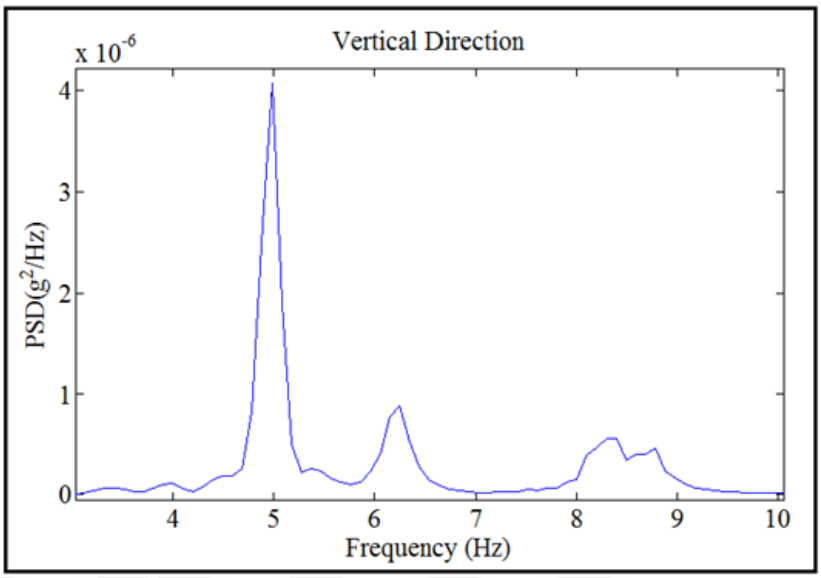

Figure 3.12. Power Spectral Density of The Bridge In The Vertical Direction.

Table 3.5. Comparison of the frequencies in the transverse direction.

	Modal Analysis	Non-updated FEM	Difference %
Mode 1	6.12 Hz	6.73 Hz	9.06
Mode 2	10.45 Hz	9.86 Hz	5.65
Mode 3	15.82 Hz	13.91 Hz	12.07

Table 3.6. Comparison of the frequencies in the longitudinal direction.

	Modal Analysis	Non-updated FEM	Difference %
Mode 1	5.10 Hz	6.36 Hz	24.70
Mode 2	6.35 Hz	6.95 Hz	9.45

Table 3.7. Comparison of the frequencies in the vertical direction.

	Modal Analysis	Non-updated FEM	Difference %
Mode 1	4.98 Hz	5.11 Hz	2.61
Mode 2	6.12 Hz	5.88 Hz	3.92
Mode 3	8.69 Hz	7.25 Hz	16.57

Figure 3.11 and 3.12 show power spectra of the first singular values in the transverse and longitudinal directions respectively. Comparisons of frequencies obtained by modal analysis and non-updated FEM in the transverse, longitudinal and vertical directions are presented in Tables 3.5 to 3.7.

As the second step, minimization between the modal values obtained from the FEM and the measurements was performed. Error function considers modal frequencies, mode shapes and weighing coefficients depending on the confidence level of corresponding modal parameter. Simulated modal frequencies and mode shapes are obtained from eigenvalues and eigenvectors of finite element models, respectively; whereas measured modal frequencies and mode shapes are obtained from FDD. Error function, defined in equation below, characterized by bent stiffness values, is defined as

$$E(\alpha) = \sum_{i=1}^{3} (k_i.[(f_i^* - f_i)/f_i]^2 + h_i.[1 - MAC_i]^2) \tag{3.8}$$

where

α : stiffness correction coefficient

i : mode number

k_i : weighing coefficient for modal frequencies

h_i : weighing coefficient for MAC value

f_i^* : measured modal frequencies

f_i : simulated modal frequencies

MAC_i : modal assurance criteria between the mode shapes obtained from simulation and measurement

Modal Assurance Criteria defines the similarity between two mode shapes; here, it defines the similarity between the modes shapes obtained from FEM simulation and measurement. Weighing coefficients are determined to represent the confidence levels of modal parameters. Modal frequency and mode shape of the first mode should be accurately estimated as it is the primary representative of vibration characteristics of a structure. Accordingly, the first, the second and the third modal frequencies and the first mode shape are intended to have high accuracies, and k and h values are defined according to mass participation ratios of these modes. Comparisons of frequencies obtained by modal analysis and updated FEM in the transverse, longitudinal and vertical directions are presented in Tables 3.8 to 3.10 whereas figure 3.13 shows the first three mode shapes of the bridge obtained from modal analysis and updated finite element model. According to model updating, stiffness of the bridge decreased from 1.0 (the starting value which was calculated using design drawings) to 0.65. The final value is reasonable when the cracked stiffness suggested by Seismic Design Codes are considered.

Table 3.8. Comparison of the frequencies in the transverse direction.

	Modal Analysis	Updated FEM	Difference %
Mode 1	6.12 Hz	6.12 Hz	-
Mode 2	10.45 Hz	9.50 Hz	9.09
Mode 3	15.82 Hz	13.67 Hz	13.59

Table 3.9. Comparison of the frequencies in the longitudinal direction.

	Modal Analysis	Updated FEM	Difference %
Mode 1	5.10 Hz	5.92 Hz	16.08
Mode 2	6.35 Hz	6.73 Hz	5.98

Table 3.10. Comparison of the frequencies in the vertical direction.

	Modal Analysis	Updated FEM	Difference %
Mode 1	4.98 Hz	4.76 Hz	4.42
Mode 2	6.12 Hz	5.60 Hz	8.49
Mode 3	8.69 Hz	7.11 Hz	18.18

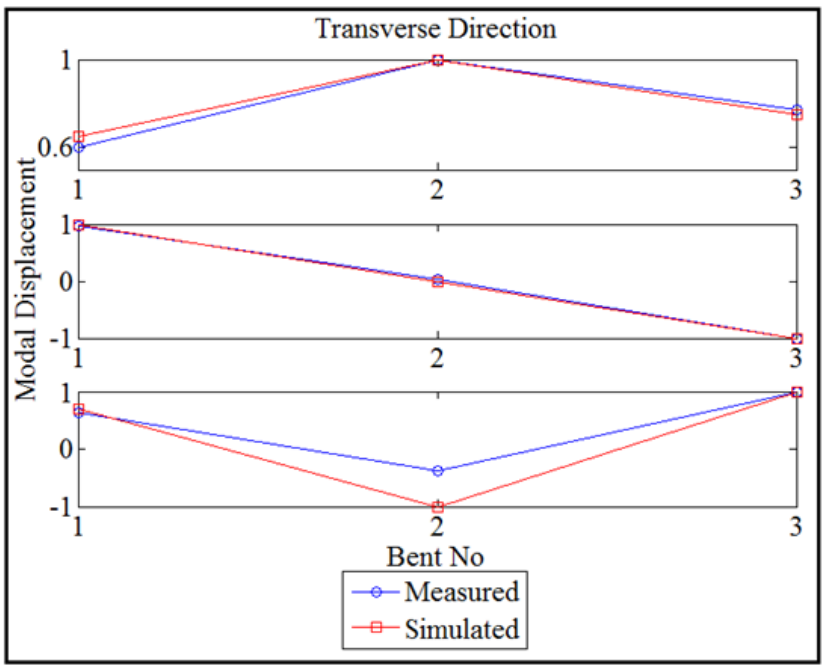

Figure 3.13. Mode Shapes of the Structure obtained from System Identification and Updated Finite Element Model.

4. CONDITION ASSESSMENT AND SEISMIC VULNERABILITY ESTIMATION OF A FOUR-SPAN BRIDGE MODEL

In this chapter, measurements of a large scale bridge experiment, carried out at University of Nevada-Reno, were used. The aim of this part was to validate the proposed system identification method for condition assessment of bridges. For this purpose, analytical model of the bridge was constructed using drawings and material properties and calibrated according to modal parameters at different damage states. The identified damage levels were compared with calculated ones using curvature measurements in order to validate the proposed methodology. Moreover, nonlinear time history analyses were carried out using earthquake excitations of experiments to observe effects of modelling uncertainties on damage detection were investigated by nonlinear analysis of 4-span bridge modelled with different hinge models.

4.1. Experimental Setup and Test Procedure

A three-bent, four-span, reinforced concrete bridge structure was exposed to a series of earthquake and white noise excitations by three shaking tables, simultaneously. The total length of the bridge deck was 32.6m. Columns' lengths were 1.58m, 2.18m and 1.88m for Bent-1, Bent-2 and Bent-3 respectively. Figure 4.1 presents the three-dimensional view of the test-setup whereas Figure 4.2 shows the dimensions of the bridge. Each bent consists of two columns with the same circular cross-section, but differs in height. As a consequence, lateral stiffness value of each bent is different, affecting transverse modal characteristics. Additional masses were anchored to the deck, to represent adjacent spans of a typical bridge structure. In total, twenty-seven accelerometers were placed at the deck of the bridge to measure vibration response in three directions throughout the tests with a sampling frequency of 128 Hz.

The bridge model was subjected to a series of acceleration records that were derived from the Century City record of the 1994 Northridge, California earthquake. The records consisted primarily of biaxial motions although some uniaxial longitudinal tests were conducted for supplemental testing. The record for the abutments seats was generated using analytical models of the bridge and abutments subjected to the test motions. The abutment motions were applied solely in the longitudinal direction assuming that the transverse abutment shear keys were sacrificial (Nelson *et al.*, 2007). The whole ground motion excitations in the transverse and longitudinal directions are illustrated in Figure 4.3 and explained in Table 4.1.

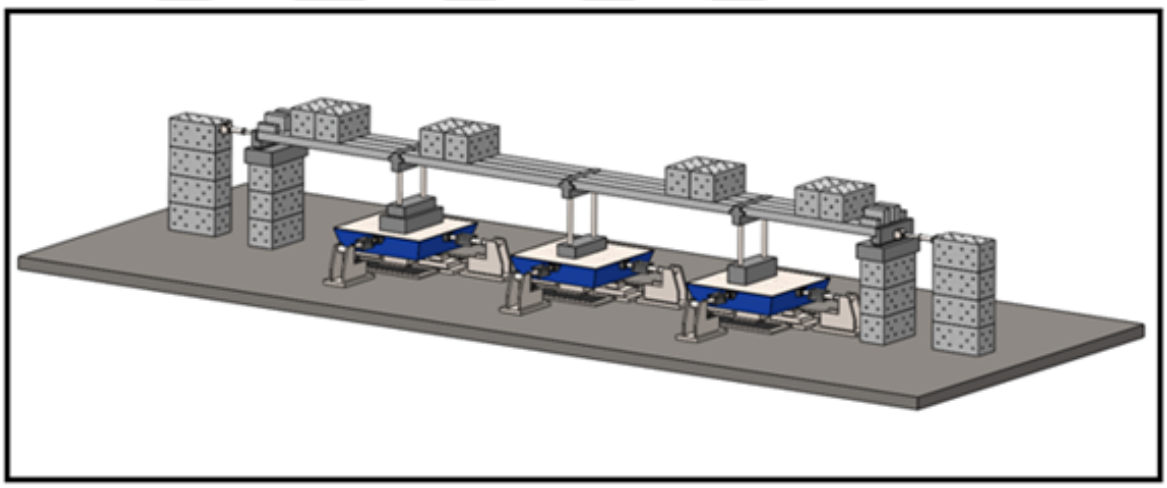

Figure 4.1. Test Setup.

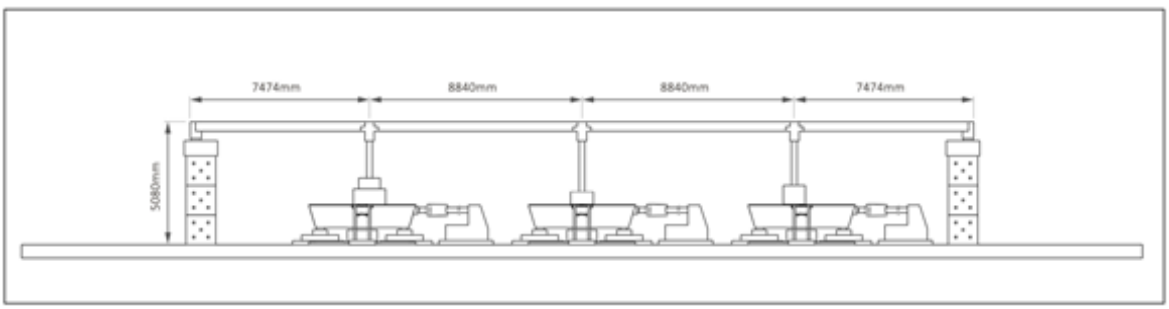

Figure 4.2. Dimensions of the Bridge.

Table 4.1. Test Procedure with Ground Motion Levels.

Test ID	Transverse PGA (g)	Longitudinal PGA (g)
1	0.07	0.09
2	0.15	0.18
3	0.25	0.30

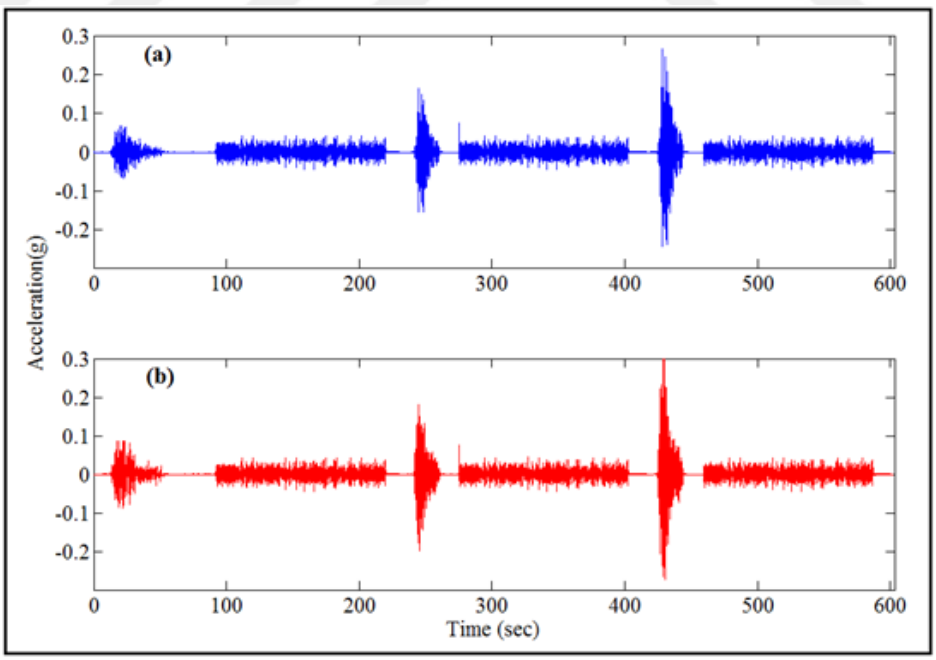

Figure 4.3. Test Procedure: (a) Transverse Direction, (b) Longitudinal Direction.

4.2. Finite Element Modelling and Nonlinear Analysis

In this section, modeling assumptions for nonlinear time history analysis are explained. In reinforced concrete bridge structures, a widely used damage indicator is rotation at column ends. Certain nonlinear modeling techniques would provide different results, and different accuracies. Definition of stiffness and strength degradation, and decision whether plasticity is concentrated or distributed plays an important role in nonlinear analysis (Aviram *et al.*, 2008). In this study, nonlinearity was modeled with two different methods. The first one is plastic hinges which represent concentrated plasticity at upper and lower column-end regions. P-M interaction of cross-section was developed using XTRACT (Chadwell and Imbsen, 2004) according to design drawings and identified stiffness value at the undamaged state. Figure 4.4 shows the cross-sectional properties and the P-M interaction of columns. The second method is the Fiber hinge model which computes moment-curvature relation in any bending direction for varying levels of axial load throughout a static or dynamic analysis. This interaction between biaxial moment and axial force, and the distribution of inelastic action throughout the section is obtained automatically by assigning particular stress-strain relationships to individual discretized fibers in the cross section. (Aviram *et al.*, 2008). Figure 4.5 presents the fiber hinge model and moment-rotation response of bent-1 during the second test.

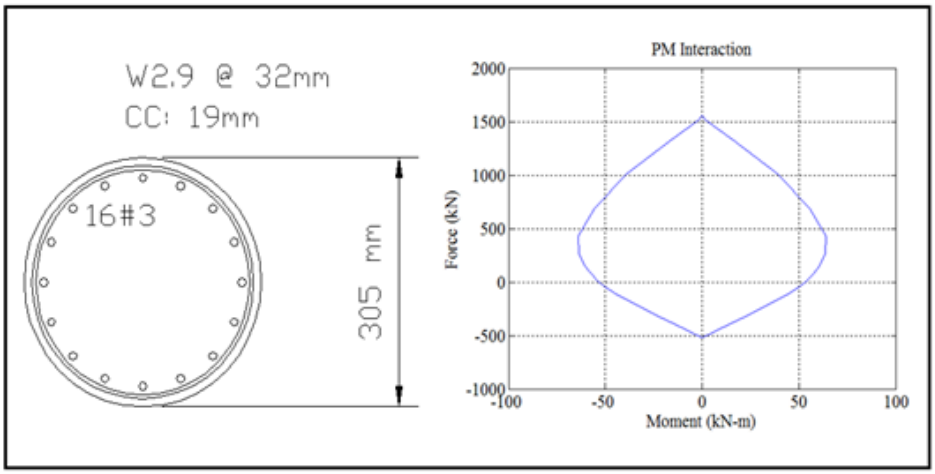

Figure 4.4. The Cross-Sectional Properties and P-M Interaction of Columns.

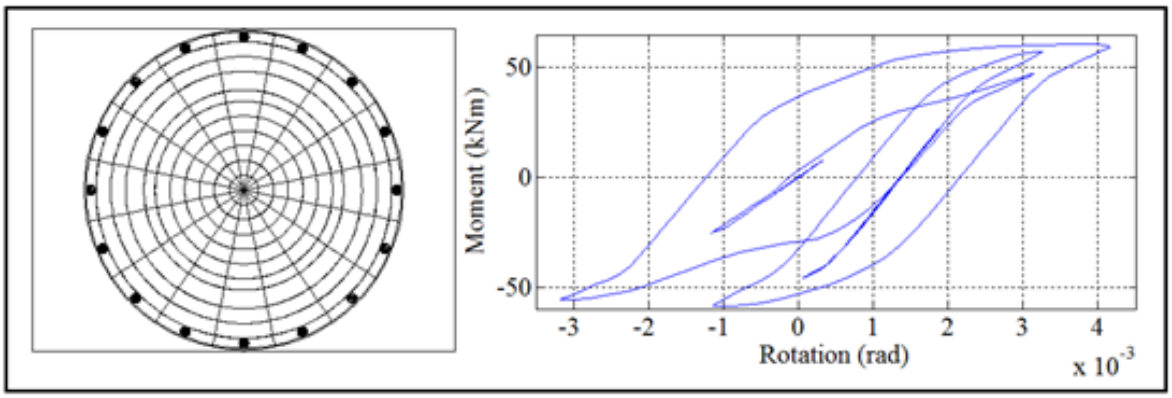

Figure 4.5. Fiber Hinge Model and Moment-Rotation Response (Test-2).

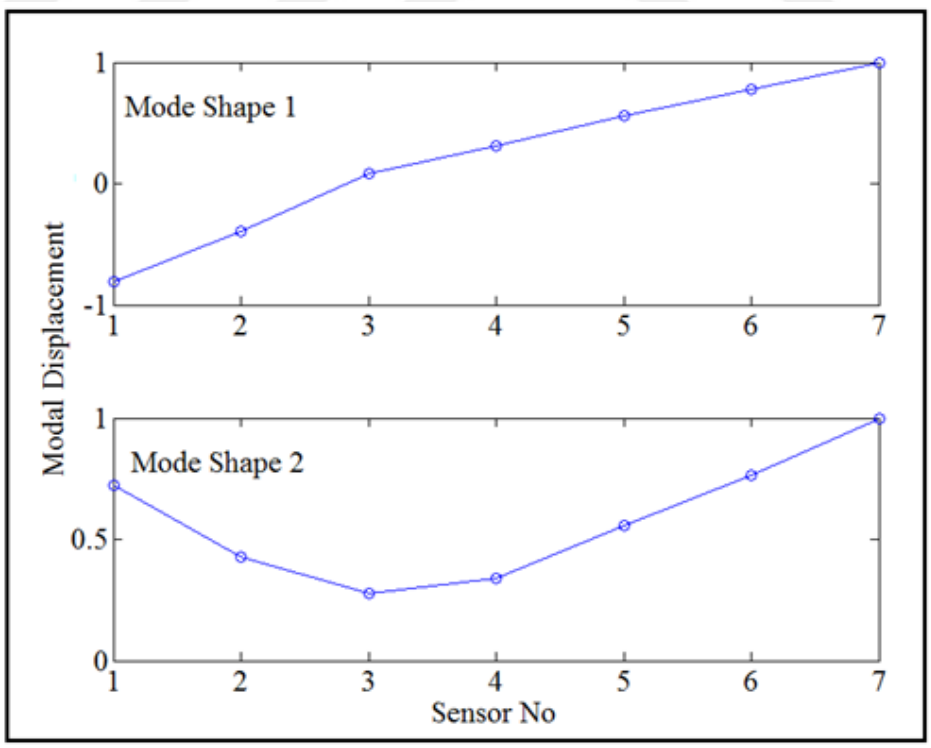

Figure 4.6. Identified Mode Shapes of the Bridge under Test-1.

The bridge-abutment interaction was provided by the actuators at two ends of the structure. In the nonlinear time history analysis, the actuator forces measured during the tests were assigned as point loads at the abutment locations. Column bases were assumed to be fixed because they will be rigidly attached to the shake tables. In order to make a fair comparison between the damage progress obtained from identification and FEM analysis, material properties of the structure at undamaged state are taken from the FEM update which will be explained in the next section. In other words, finite element model that satisfies the identification results of the initial state were used in the nonlinear time history analysis. The only difference is that in the FEM analysis abutment points are considered as free in the transverse direction because the identification results of Test-1 shows that the friction between deck and concrete block is eliminated under an earthquake excitation. Figure 4.6 presents the first two mode shapes of the structure under a strong motion.

Equations 4.1, 4.2, 4.3 and 4.4 relate the sectional moment curvature behavior with effective stiffness. Yield curvature could be interpreted in terms of yield rotation such as

$$\phi_y = \frac{\Theta_y}{L_p} \tag{4.1}$$

where

ϕ_y : yield curvature

Θ_y : yield rotation

L_p : plastic hinge length

A relationship between stiffness and moment-curvature could be established through such as

$$EI = \frac{M}{\sigma} \tag{4.2}$$

where

EI: initial stiffness

E : modulus of elasticity

M : moment of inertia

M : moment

σ : curvature

which could be used to define effective stiffness in terms of initial stiffness and ductility (Priestley, 1996) such as

$$EI_{eff} = \frac{EI}{\mu} \tag{4.3}$$

$$\mu = \frac{\sigma_{max}}{\sigma_y} \tag{4.4}$$

where

EI_{eff} : effective stiffness

μ : ductility

σ_{max} : the maximum rotation

In other words, after a damaging earthquake event, the stiffness of the damaged region, and the primary stiffness of moment-rotation behavior would be inversely proportional with damage severity designated with ductility. The earthquake moves as a single wave and when it reaches the bridge with an angle of δ, the structure is shaken by two components with magnitudes $M\cos(\delta)$ and $M\sin(\delta)$ in longitudinal and transverse directions,respectively (Banerjee Basu and Shinozuka, 2011). The dynamic response of the bridge at an arbitrary location and time instant t is $\theta(t)$.

This response can either be bridge deformation or a resultant force. In this study, rotations at column ends were used to predict damage progress of the structure. The maximum rotation was obtained from equations 4.5 and 4.6.

$$\theta(t) = \theta_L(t\cos(\delta) \ + \theta_T(t\sin(\delta) \tag{4.5}$$

$$\theta_{max} = \max\theta(t) \tag{4.6}$$

where

$\theta_L(t)$: rotation in the longitudinal direction at time instant t

$\theta_T(t)$: rotation in the transverse direction at time instant t

Table 4.2. Comparison between Effective Stiffness Values Obtained using Two Hinge Models (Bent-1).

Damage State	Plastic Hinge	Fiber Hinge	Difference %
State 1	1.00	1.00	-
State 2	0.60	0.56	7.14
State 3	0.37	0.42	11.90

Table 4.3. Comparison between Effective Stiffness Values Obtained using Two Hinge Models (Bent-2).

Damage State	Plastic Hinge	Fiber Hinge	Difference %
State 1	1.00	1.00	-
State 2	0.90	0.85	5.88
State 3	0.50	0.80	37.50

The comparison between effective stiffness values obtained using plastic hinges and fiber hinges are presented in Tables 4.2 to 4.4 for bent-1, bent-2 and bent-3, respectively. The difference varies from 11.90% to 40.4%. Although other parameters are exactly same for two models, the different methods used to represent the hysteretic behavior of columns result significant differences in predicted final conditions of the bridge.

Table 4.4. Comparison between Effective Stiffness Values Obtained using Two Hinge Models (Bent-3).

Damage State	Plastic Hinge	Fiber Hinge	Difference %
State 1	1.00	1.00	-
State 2	0.50	0.56	10.71
State 3	0.25	0.42	40.48

4.3. System Identification and Finite Element Model Updating

In this section, system identification is carried out in frequency domain using vibration measurements of white noise excitations. The identification strategy is based on the fact that the system is linear time-invariant, which means that structure experiences no damage-change throughout the observation. In order to obtain the initial and final conditions of the bridge, a finite element model was developed according to design drawings. Afterwards, a FEM updating procedure was carried out to minimize the difference between the dynamic properties of the model and of the real structure. For this purpose, many finite element models were created by changing the updated parameters and the dynamic properties of each model were stored. Finally, an error function was used to minimize the difference between frequencies and mode shapes obtained from simulations and measurements. In other words, the most representative FEM was selected to assess the condition of the bridge at different states.

Initial finite element model was constructed using SAP2000 V15 with frame elements based on design drawings. Inspecting the structural system, it is expected that the deck would experience almost no damage, while the vast amount of damage will occur on the columns and generally on the column ends. In other words, parameters which are the major sources of change in the structural system are the stiffness values of the columns.

The states of a structure were defined as the initial state, and the damaged states. In the initial state, where no damage was expected, system identification was conducted for determining the stiffness of bent as a whole, as each portion of the column would have the same material and sectional properties. The first mode shape of structure showed that there was a friction between deck and concrete blocks at abutment locations. Therefore, two linear links were assigned in the transverse direction to represent the effect of friction and their stiffness values were also identified. Hence, at the initial state, three updating parameters; $\alpha_1, \alpha_2, \alpha_3$, were representing the stiffness modification factor of all columns and stiffness values of links assigned to two end of the bridge, respectively. At damaged state, identification was carried out only for the column-ends as the major damage is expected at those regions. Therefore, at this part, three updating parameters $\beta_1, \beta_2, \beta_3$, are representing the stiffness modification factors of bent-1, bent-2 and bent-3, respectively.

Structural parameter identification in the frequency domain has two steps. The first step is the identification of the modal values using the acceleration measurements of the bridge. The second step is the minimization of the error between the modal values obtained from the FEM and the measurements. An output-only method, the Frequency Domain Decomposition (FDD) method (e.g., Otte *et al.*, 1990; Brincker *et al.*, 2001) was used to extract modal parameters from the vibration measurements without requiring information for input. Figure 4.7 shows power spectra of the first singular value for different damage states. With the help of the figure, increase in structural damage could be tracked by observing the decrease in modal frequencies which are obtained as in Table 4.5. Since the total mass participation ratios of the first three modes were almost 98%, higher modes were thought as negligible and so they weren't taken into account during the model updating and condition assessment process.

As the second step, minimization between the modal values obtained from the FEM and the measurements was performed. Error function considers modal frequencies, mode shapes and weighing coefficients depending on the confidence level of cor-

responding modal parameter. Equations 4.7 and 4.8 show the error functions used at the undamaged and damaged states, respectively.

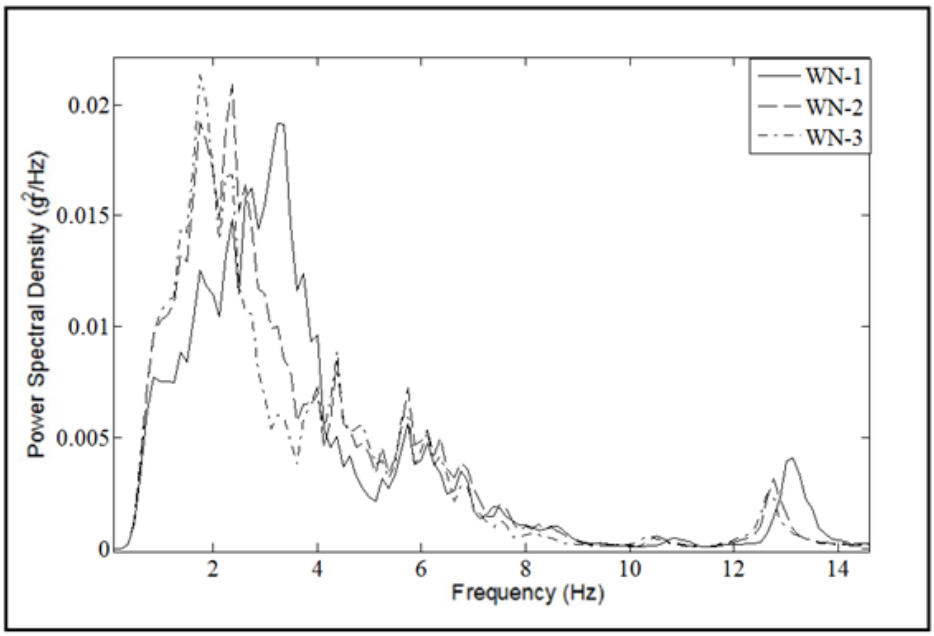

Figure 4.7. Power Spectra of the First Singular Value at Different Damage States.

Table 4.5. Identified Natural Frequencies.

Motion	Mode 1	Mode 2	Mode 3
WN 1	3.37 Hz	6.13 Hz	13.13 Hz
WN 2	2.75 Hz	5.75 Hz	12.75 Hz
WN 3	2.38 Hz	4.38 Hz	12.60 Hz

$$E(\alpha_1, \alpha_2, \alpha_3) = \sum_{i=1}^{3} (k_i.[(f_i^* - f_i)/f_i]^2 + h_i.[1 - MAC_i]^2) \tag{4.7}$$

$$E(\beta_1, \beta_2, \beta_3) = \sum_{i=1}^{3} (k_i.[(f_i^* - f_i)/f_i]^2 + h_i.[1 - MAC_i]^2) \tag{4.8}$$

where

α : stiffness correction coefficient

i : mode number

k_i : weighing coefficient for modal frequencies

h_i : weighing coefficient for MAC value

f_i^* : measured modal frequencies

f_i : simulated modal frequencies

MAC_i : modal assurance criteria between the mode shapes obtained from simulation and measurement

Tables 4.6 to 4.8 have the comparison of modal frequencies obtained from system identification and finite element model updating. Figure 4.8 presents the first three mode shapes of the bridge obtained from identification and updated finite element model.

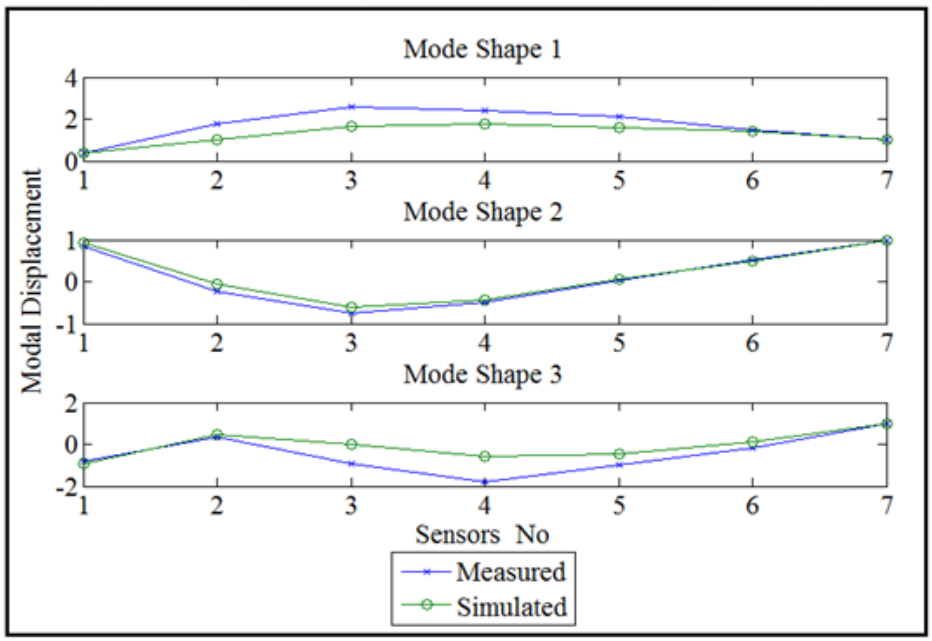

Figure 4.8. Mode Shapes of the Structure obtained from System Identification and Updated FEM.

Table 4.6. The Comparison of the Modal Frequencies of the Updated and Non-updated FEMs with Identified ones for Damage State-1 (WN1).

	System Identification	Non-Updated FEM	Difference %	Updated FEM	Difference %
WN 1	3.37 Hz	4.45 Hz	32.05	3.36 Hz	0.29
WN 2	6.13 Hz	7.69 Hz	25.45	5.85 Hz	4.56
WN 3	13.13 Hz	13.99 Hz	6.55	10.08 Hz	23.23

Table 4.7. The Comparison of the Modal Frequencies of the Updated and Non-updated FEMs with Identified ones for Damage State-2 (WN2).

	System Identification	Updated FEM	Difference %
WN 1	2.75 Hz	2.78 Hz	1.08
WN 2	5.75 Hz	5.13 Hz	10.78
WN 3	12.75 Hz	19.58 Hz	24.86

Table 4.8. The Comparison of the Modal Frequencies of the Updated and Non-updated FEMs with Identified ones for Damage State-3 (WN3).

	System Identification	Updated FEM	Difference %
WN 1	2.38 Hz	2.39 Hz	0.42
WN 2	4.38 Hz	5.06 Hz	15.52
WN 3	12.60 Hz	9.51 Hz	24.52

4.4. Identified and Predicted Damage Progress

This section summarizes a damage progress throughout the excitation tests, based on two different approaches; which are identification and nonlinear analysis. As it is emphasized in the previous sections, the initial models of two approaches were the updated FEM at the undamaged state. Structural identification is based on modal analysis and FEM updating, whereas the second approach involves nonlinear time history analysis for damage detection at a certain state. In other words, both approaches intend to determine modification factors for structural parameters starting from the same point. Figure 4.9 shows the effective stiffness values obtained from system identification, curvature measurements and nonlinear time history analyses for different damage states. Damage states were introduced as 1, 2, and 3; and, they correspond to the states of white noise excitations of WN1, WN2, WN3; respectively. Alternatively, they refer to the initial state, and the states after earthquake excitations of Test-2 and Test-3; respectively. Updated parameters are obtained using white noise excitations, whereas predicted parameters are obtained using earthquake excitations. The numerical comparisons of effective stiffness values are presented in Tables 4.9 to 4.11 for Bent-1, Bent-2 and Bent-3, respectively.

Table 4.9. Comparison of Identified and Predicted Stiffness Values of Bent-1.

Bent-1	Vibration Based	Plastic Hinge	Difference %	Fiber Hinge	Difference %
Pre-EQ (WN1)	1.0	1.0	-	1.0	-
Post-EQ (WN3)	0.32	0.37	15.6	0.42	31.2

Table 4.10. Comparison of Identified and Predicted Stiffness Values of Bent-2.

Bent-1	Vibration Based	Plastic Hinge	Difference %	Fiber Hinge	Difference %
Pre-EQ (WN1)	1.0	1.0	-	1.0	-
Post-EQ (WN3)	0.90	0.50	44.4	0.80	11.1

Table 4.11. Comparison of Identified and Predicted Stiffness Values of Bent-3.

Bent-1	Vibration Based	Plastic Hinge	Difference %	Fiber Hinge	Difference %
Pre-EQ (WN1)	1.0	1.0	-	1.0	-
Post-EQ (WN3)	0.18	0.25	38.9	0.54	200

In order to validate the proposed damage detection method, maximum and minimum curvature values of each bent during strong motions were used (Nelson *et al.*, 2007). The maximum rotation levels were calculated using the highest curvature measurements during earthquake excitations and ductility levels were obtained by the comparison of maximum rotation values with the yield rotation value of the cross-section. Finally, the damage levels were determined according to these ductility levels and compared with the effective stiffness obtained by presented vibration-based identification method. Tables 4.12 to 4.14 present the comparison of damage levels for bent1, bent-2 and bent-3, respectively. In this study, six damage levels are considered, whose ductility demand intervals are listed in Table 4.15 (Banerjee and Shinozuka, 2008). Results indicate that identified stiffness values are capable of representing the actual damage levels of three bents. Therefore, it can be concluded that the presented method is capable of assessing the structural condition.

Stiffness values predicted by both Plastic hinge and Fiber hinge models differ significantly from vibration-based identified values. For instance, the minimum and the maximum differences for Plastic hinge model are 15.6% and 44.4%, respectively. The minimum difference obtained by Fiber hinge model is 11.1% for bent-2 whereas the effective stiffness value of bent-3 is three times of the identified one. These differences are too significant to be neglected since the decision of whether a structure may be demolished or not is made according to the severity of damage after an earthquake. On the other hand, Figure 4.9 indicates that the vibration-based results are very close the stiffness values obtained by curvature measurements.

Table 4.12. Comparison of Effective Stiffness of Bent-1 with Damage Levels.

Bent-1	Rotation (rad)	Ductility	Damage Level	Vbiration-Based
T2	0.013	3.73	Moderate	0.52
T3	0.020	5.60	Moderate	0.32

Table 4.13. Comparison of Effective Stiffness of Bent-2 with Damage Levels.

Bent-1	Rotation (rad)	Ductility	Damage Level	Vbiration-Based
T2	0.002	0.64	None	1.0
T3	0.004	1.10	Almost None	0.90

Table 4.14. Comparison of Effective Stiffness of Bent-3 with Damage Levels.

Bent-1	Rotation (rad)	Ductility	Damage Level	Vbiration-Based
T2	0.004	1.27	Almost None	1.0
T3	0.023	6.27	Major	0.18

Table 4.15. Rotational ductility limits.

Damage Level	Ductility Demand
None	$\mu < 1.0$
Almost None	$1.0 < \mu < 1.52$
Minor	$1.52 < \mu < 3.10$
Moderate	$3.10 < \mu < 5.72$
Major	$5.72 < \mu < 8.34$
Collapse	$8.34 < \mu$

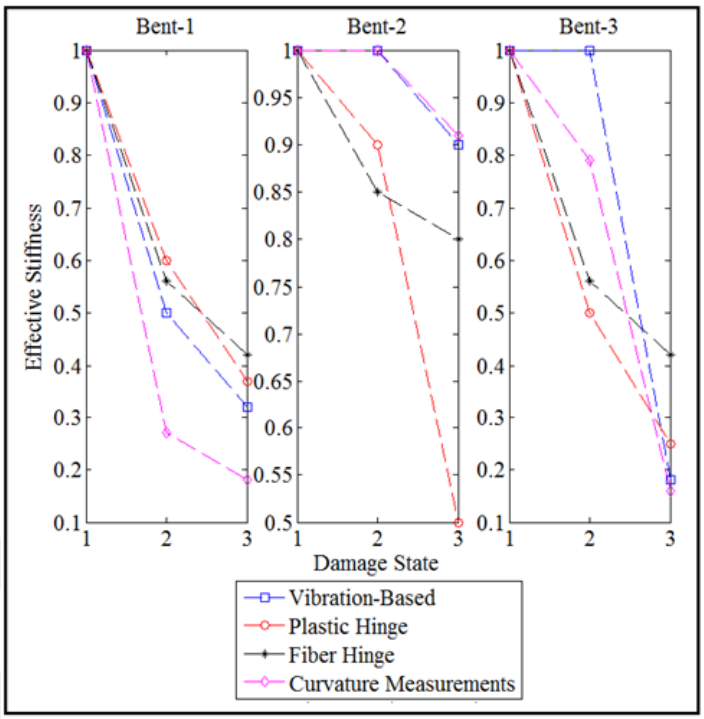

Figure 4.9. Comparison of Identified and Predicted Effective Stiffness.

4.5. Seismic Vulnerability Estimation

In this study, seismic vulnerability estimation is achieved by obtaining fragility curves (FC) for each damage states. Fragility curves are developed using two modelling approaches in order to investigate the effect of hinge properties on evaluated remaining capacity.

By means of fragility curves, the failure probability can be obtained as a function of one intensity measure. Earthquake excitations are considered as one of the major source of uncertainties for the seismic vulnerability estimation. Therefore, the randomness in earthquakes is simulated by taking into account the input motions with different peak ground acceleration (PGA) values. The development of fragility curves is based on a data set of failure probabilities with respect to PGA. In other words, the fragility curve is a cumulative density function fitting this set of data using maximum likelihood estimation. It is characterized by mean and standard deviation, and the estimation of these parameters is the ultimate objective of the procedure.

Failure probability of the structure refers to whether the ductility demand exceeds the threshold value. In the development of fragility curves, nonlinear time history analysis for a specific ground motion input returns a ductility value. By comparing this value with the threshold, one can determine the existence of damage, which is represented by 0 or 1. Several fragility curves can be developed to represent different damage levels. In this study, six damage levels are considered, whose ductility demand intervals are listed in Table 4.12 (Banerjee and Shinozuka, 2008).

There are two different methods to obtain fragility curves. The first method determines fragility curves of each damage state separately, on the other hand the second method considers the dependence of fragility curves of different damage states to each other. In the first method, there is a possibility for fragility curves of different damage levels to intersect, which is undesirable. Therefore, the second method is used and the probabilities of different damage levels are evaluated with equations 4.9 to 4.14;

$$P_{i1} = 1 - F_1(a_i, c_1, \sigma) \tag{4.9}$$

$$P_{i2} = F_1(a_i, c_1, \sigma) - F_2(a_i, c_2, \sigma) \tag{4.10}$$

$$P_{i3} = F_2(a_i, c_2, \sigma) - F_3(a_i, c_3, \sigma) \tag{4.11}$$

$$P_{i4} = F_3(a_i, c_3, \sigma) - F_4(a_i, c_4, \sigma) \tag{4.12}$$

$$P_{i5} = F_4(a_i, c_4, \sigma) - F_5(a_i, c_5, \sigma) \tag{4.13}$$

$$P_{i5} = F_5(a_i, c_5, \sigma) \tag{4.14}$$

where

c_1, c_2, c_3, c_4, c_5 : mean values of the first, second, third, fourth, and fifth fragility curves

σ : standard deviation of fragility curves

a_i : the PGA of ith input ground motion

Maximum likelihood estimation is performed by equation 4.15

$$L(c_1, c_2, c_3, c_4, c_5) = \prod_{i=1}^{110} \prod_{k=1}^{6} P(a_i, E_k)^{x_{ik}} \tag{4.15}$$

where

i : the number of dynamic analyses performed with different input ground motions

k : the number of fragilities (probabilities) evaluated at ith analysis (PGA)

$x_{ik} = 1$ when damage state $E_k$occurs for ith analysis subjected to $a = a_i$

$x_{ik} = 0$ when damage state $E_k$does not occur for ith analysis subjected to $a = a_i$

To create a data set of failure probabilities, each corresponding to a PGA, nonlinear time history analyses are carried out in which ground motion input is the varying parameter. 110 ground motion records of the Northridge earthquake (1994) are selected from the Pacific Earthquake Engineering Research Center (PEER) database. Finally, fragility curves based on models with different hinge properties are developed.

Figures 4.10 to 4.12 present the fragility curves for minor, moderate, and major damage at damage states 1, 2 and 3, respectively. It can be observed that at a given damage state, the probabilities of failure obtained using plastic and fiber hinges are different.

Tables 4.16 to 4.18 give certain representative values for the failure probabilities at different damage states in order to clarify the finding from figures. For instance, at the final damage state, difference of failure probabilities for minor (at 0.2g), moderate

(at 0.4g) and major (at 0.6) damages are 9.3%, 5.6% and 9.4%, respectively. It is also indicated that the difference in the seismic vulnerability estimations of two models is increased as damage progresses in the structure. For example, difference of failure probabilities for major damage is increased from 3.7% to 9.4%. Similarly, for moderate damage, difference is increased from 1.68% to 5.6%.

Table 4.16. Comparison of Failure Probabilities at Damage State 1.

Damage State-1	Minor FC (0.2g)	Moderate FC (0.4g)	Major FC (0.6g)
Plastic Hinge	0.513	0.723	0.722
Fiber Hinge	0.687	0.711	0.696

Table 4.17. Comparison of Failure Probabilities at Damage State 2.

Damage State-1	Minor FC (0.2g)	Moderate FC (0.4g)	Major FC (0.6g)
Plastic Hinge	0.578	0.763	0.751
Fiber Hinge	0.693	0.730	0.715

Table 4.18. Comparison of Failure Probabilities at Damage State 3.

Damage State-1	Minor FC (0.2g)	Moderate FC (0.4g)	Major FC (0.6g)
Plastic Hinge	0.634	0.804	0.789
Fiber Hinge	0.699	0.761	0.721

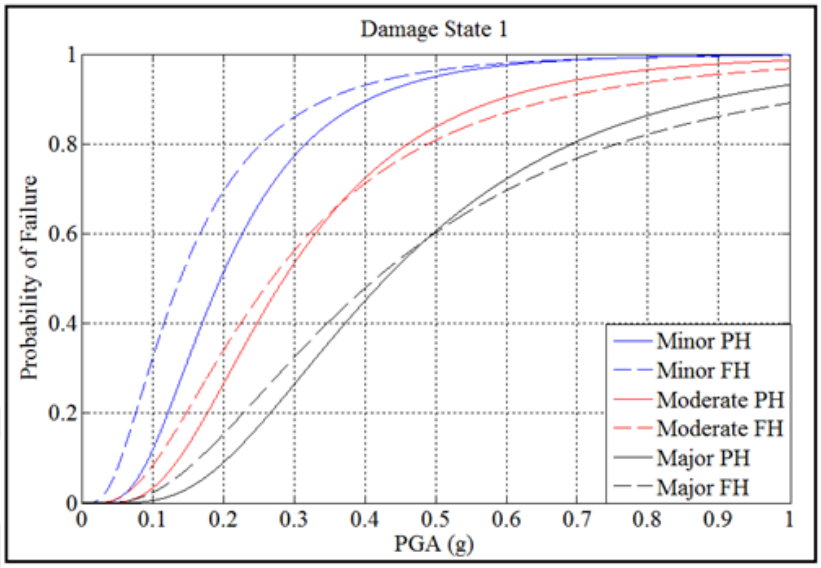

Figure 4.10. Comparison of Fragility Curves at Damage State-1.

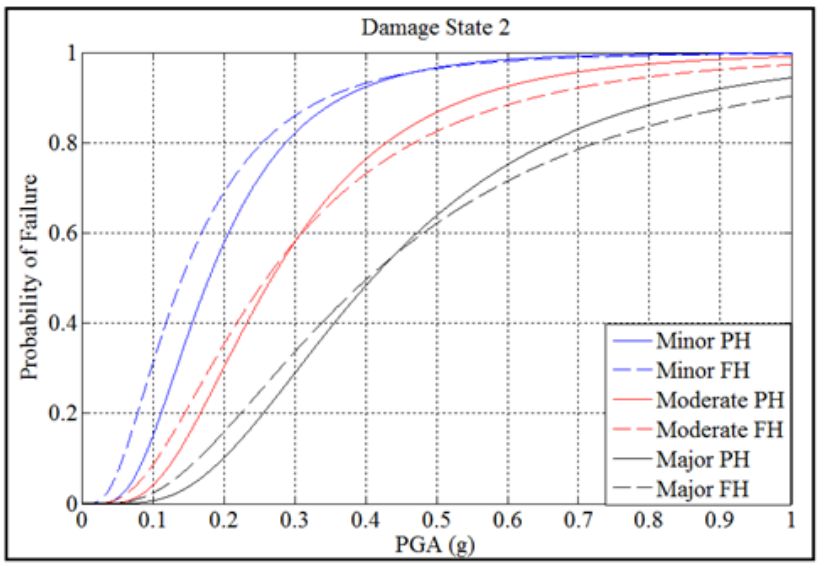

Figure 4.11. Comparison of Fragility Curves at Damage State-2.

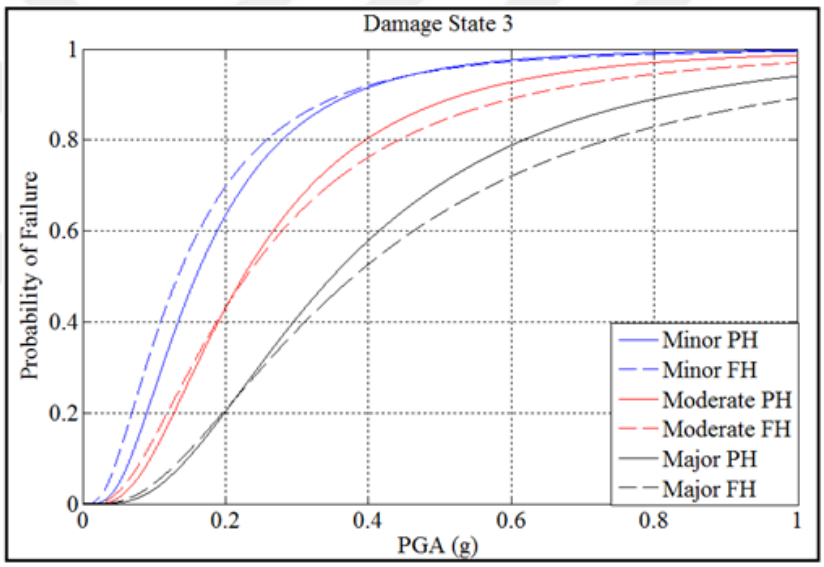

Figure 4.12. Comparison of Fragility Curves at Damage State-3.

5. CONCLUSION

In this study, implementation of structural health monitoring and structural identification of reinforced concrete highway bridges are conducted and effects of hinge properties on condition assessment and seismic vulnerability estimation are investigated. For this purpose, vibration measurements of two structures are used. The first one is Etiler bridge located in Istanbul and the other structure is a four-span three-bent bridge model tested at University of Nevada-Reno. Stiffness values of both structures are determined based on vibration-based identified structural parameters in frequency domain and the identification results of the experimental model are validated using curvature measurements. Finally, effects of hinge modelling on condition assessment and reliability estimation are investigated by nonlinear time history analysis of the second bridge. The conclusions and recommendations for future studies are presented followings:

- Long-term monitoring and system identification of vibration measurements indicated that structural conditions of Etiler bridge did not change within almost two years. The reason of this situation may be that since the bridge is very young the deterioration process may not have been started yet. Therefore, if the monitoring of structure would continue in the future, changes in modal frequencies due to aging will be measured and it will also give an interesting opportunity to investigate the rate of bridge aging in different periods of its life.

- Before stiffness of Etiler bridge was determined via vibration-based system identification, a study about the effects of modelling simplifications of abutments and footings of the structure on its dynamic characteristic were carried out and simplified models were improved using empirical equations. Since different empirical equations suggested by different researchers are available in the literature, a parametric study may be conducted, using identification and nonlinear analysis, to investigate their accuracies and effects on analytical simulations.

• In the fourth chapter of this study, system identification method used for Etiler bridge was validated via measurements of a large-scale bridge experiment. Moreover, a parametric study on effects of different nonlinear modelling approaches on condition assessment and seismic vulnerability estimation of reinforced concrete bridges was carried out. In the condition assessment part, it was clearly observed that stiffness values predicted by nonlinear analyses are different from not only each other but also identified and calculated results. Therefore, a study on nonlinear modelling, especially nonlinear damping, of bridges may be valuable to improve analytical results.

• Seismic vulnerability estimation of the bridge, tested at University of Nevada-Reno, was achieved by fragility curves developed based on a set of earthquake records which belong to 1994 Northridge Earthquake. Therefore, another set of records could lead different results. For this purpose, different sets of records could be used to observe the differences. Such differences could be related with strong ground motion parameters which enables to achieve a generalized solution. Therefore, a parametric study on input uncertainties would be an interesting topic and it would give worthwhile results about the effects of input selection on the reliability estimation.

• Finally, in the nonlinear time history analysis of Reno bridge for condition assessment and seismic vulnerability estimation, moment curvature behavior of columns was defined at the initial (undamaged) state. Therefore, it must be noted that if nonlinear behavior of columns is defined at different damage states, results of computer simulations would change. Moreover, for the fiber hinge model, cross-section of the columns is also defined at the initial (undamaged) state. Therefore, change in the cross-section due to damage must also be reflected in this model in order to have more realistic results from nonlinear analysis.

REFERENCES

ACI Committee 318, 2008, "Building Code Requirements for Structural Concrete and Commentary", American Concrete Institute, Farmington Hills, MI.

Akgul, F. and D.M., Frangopol, 2004, "Lifetime Performance Analysis of Existing Prestressed Concrete Bridge Superstructures", Journal of Structural Engineering, Vol. 130, No. 12, pp. 1889-1903

Altunisik, A.C., A., Bayraktar, and Sevim, B., 2013, "Analytical and experimental Modal Analyses of a Highway Bridge Model", Computers and Concrete, Vol. 12, No. 6, pp. 803-818.

Altunisik, A.C., A., Bayraktar, B., Sevim, and F., Birinci, 2011, "Vibration-Based Operational Modal Analysis of the Mikron Historic Arch Bridge After Restoration", Civil Engineering and Environmental Systems, Vol. 28, No. 3, pp. 247-259.

Aviram A., K.R., Mackie and B., Stodjadinovic, 2008, Peer Reports 2008/03 Guidelines for Nonlinear Analysis of Bridge Structures in California.

Bandara, R.P., T.HT., Chan, and D.P., Thambiratnam, 2014, "Structural Damage Detection Method using Frequency Response Functions", Structural Health Monitoring, Vol. 13, No. 4, pp. 418-429.

Banerjee, B.S. and M., Shinozuka, 2008, "Experimental Verification of Bridge Seismic Damage States Quantified by Calibrating Analytical Models with Empirical Field Data", Earthquake Engineering and Engineering Vibration, Vol. 7, No. 4, pp. 383-393.

Banerjee B.S., and M., Shinozuka, 2011, "Effect of Ground Motion Directionality on Fragility Characteristics of a Highway Bridge", Advances in Civil Engineering, Hindawi Publishing Corporation, Volume 2011, Article ID 536171.

Bardakis, V.G., and S.E., Dritsos, 2007, "Evaluating Assumptions for Seismic Assessment of Existing Buildings", Soil Dynamics and Earthquake Engineering, No. 27, 223-233.

Bayraktar, A., A.C., Altunisik, B., Sevim, T., Turker, A., Domanic, and Y., Tas, 2009, "Vibration Characteristics of Komurhan Highway Bridge Constructed with Balanced Cantilever Method", Journal of Performance of Constructed Facilities, Vol. 23, No. 2, pp.90-99.

Beck, J.L., and L.S., Katafygiotis, 1998, "Updating Models and Their Uncertainties. I: Bayesian Statistical Framework", Journal of Engineering Mechanics, Vol. 124, No. 4, pp.455-461.

Belleri, A., B., Moaveni, and J.I., Restrepo, 2014, "Damage Assessment through Structural Identification of a Three-Story Large-Scale Precast Concrete Structure", Earthquake Engineering and Structural Dynamics, No. 43, pp. 61-76.

Brincker, R., L., Zhang, and P., Andersen, 2001, "Modal Identification of Output-Only System Using Frequency Domain Decomposition", Smart Materials and Structures, Vol. 10, No. 3, pp. 441-455.

Brownjohn, J.M.W., 2007, "Structural Health Monitoring of Civil Infrastructure", Philosophical Transactions of the Royal Society, Vol. 3, No. 65, pp. 589-622.

Brownjohn, J.M.W., P., Moyo, P., Omenzetter, and Y., Lu, 2003, "Assesment of Highway Bridge Upgrading by Dynamic Testing and Finite-Element Model Updating", Journal of Bridge Engineering, Vol. 8, No. 3, pp. 162-172.

Brownjohn, J.M.W., P., Moyo, P., Omenzetter, and S., Chakraborty, 2005, "Lessons from Monitoring the Performance of Highway Bridges", Structural Control and Health Monitoring, No. 12, pp. 227-244.

Caltrans (2013). Caltrans Seismic Design Criteria version 1.7. California Department of Transportation, Sacramento, California.

Carden, E.P., and P., Fanning, 2004, "Vibration-Based Condition Monitoring-A Review", Structural Health Monitoring, Vol. 3, No. 4, pp. 355-377.

Catbas, F.N., M., Susoy and D.M., Frangapol, 2008, "Structural Health Monitoring and Reliability Estimation: Long Span Truss Bridge Application with Environmental Monitoring Data", Engineering Structures, No. 30, pp. 2347-2359.

Celarec, D., and M., Dolsek, 2013, "The Impact of Modelling uncertainties on the Seismic Performance Assessment of Reinforced Concrete Frame Buildings", Engineering Structures, No. 52, pp. 340–354.

Chadwell, C. and R. Imbsen, 2004, "XTRACT: A Tool for Axial Force - Ultimate Curvature Interactions", Structures 2004, pp. 1-9.

Chen, Y.C., M.Q., Feng, and C.A., Tan, 2009, "Bridge Structural Condition Assessment Based on Vibration and Traffic Monitoring", Journal of Engineering Mechanics, Vol. 135, No. 8, pp. 747-758.

Dackermann, U., W.A., Smith, and R.B., Randall, 2014, "Damage Identification based on Response-only Measurements using Cepstrum Analysis and Artificial Neural Network", Structural Health Monitoring, Vol. 13, No. 4, pp. 430-444.

Doebling S.W., C.R., Farrar, M.B., Prime and D. W., Shevitz, 1996, "Damage Identification and Health Monitoring of Structural and Mechanical Systems from Changes in Their Vibration Characteristics:A Literature Review", Los Alamos National Laboratory Report, LA-13070 MS.

Enright, M.P., and D.M., Frangopol, 1998, "Service-Life Prediction of Deteriorating Concrete Bridges", Journal of Structural Engineering, Vol. 124, No. 3, pp. 309-317.

Ergun, S., and A., Demir, 2014, "Effect of Hysteretic Models on Seismic Behavior of Existing RC Structures", Journal of Performance of Constructed Facilities, Vol. 29, No. 6.

Eslami, A., and H.R., Ronagh, 2014, "Effect of Elaborate Plastic Hinge Definition on the Pushover Analysis of Reinforced Concrete Buildings", The Structural Design of Tall and Special Buildings, No. 23, pp. 254–271.

Farrar, C.R., and G.H., James, 1997, "System Identification from Ambient Vibration Measurement on a Bridge", Journal of Sound and Vibration, No. 205, pp. 1-18.

Feng, M.Q., D.K., Kim, J.H., Yi, and Y., Chen, 2004, "Baseline Models for Bridge Performance Monitoring", Journal of Engineering Mechanics, Vol. 130, No. 5, pp. 562-569.

Frangopol, D.M., A., Strauss and S., Kim, 2008, "Bridge Reliability Assessment Based on Monitoring", Journal of Bridge Engineering, Vol. 13, No. 3, pp. 258-270.

Ghosn, M., D.M., Frangopol, T.P., McAllister, M., Shah, S.M.C., Diniz, B.R., Ellingwood, L., Manuel, F., Biodini, N., Catbas, A., Strauss and L., Zhao, 2016, "Reliability-Based Performance Indicators for Structural Members", Journal of Structural Engineering, published online.

Gomez, H.C., P.J., Fanning, M.Q., Feng, and S., Lee, 2011, "Testing and Long-Term Monitoring of a Curved Concrete Box Girder Bridge", Engineering Structures, Vol. 33, No. 10, 2861-2869.

Gomez, H.C., H.S., Ulusoy and M.Q., Feng, 2013, "Variation of Modal Parameters of a Highway Bridge Extracted from Six Earthquake Records", Earthquake Engineering and Structural Dynamics, No. 42, pp. 565-579.

Goulet, C.A., C.B., Haselton, J., Mitrani-Raiser, J.L., Beck, G.G., Deierlein, K.A., Porter, and J.P., Stewart, 2007, "Evaluation of the Seismic Performance of a Code-Conforming Reinforced-Concrete Frame Building from Seismic Hazard to Collapse Safety and Economic Losses", Earthquake Engineering and Structural Dynamics, No. 36, pp. 1973-1997.

Guan, H., and V.G., Karbhari, 2006, "Web-Based Structural Health Monitoring of an FRP Composite Bridge", Computer-Aided Civil and Infrastructure Engineering, No. 21, pp. 39-56.

Gul, M., and F.N., Catbas, 2008, "Ambient Vibration Data Analysis for Structural Identification and Global Condition Assessment", Journal of Engineering Mechanics, Vol. 134, No. 8, pp. 650-662.

Huang, C.S., S.L., Hung, C.M., Wen, and T.T., Tu, 2003, "A Neural Network Approach for Structural Identification and Diagnosis of a Building from Seismic Response Data", Earthquake Engineering and Structural Dynamics, No. 32, pp. 187-206.

Inel, M, and H.B., Ozmen, 2006, "Effects of Plastic Hinge Properties in Nonlinear Analysis of Reinforced Concrete Buildings", Engineering Structures, No. 28, pp. 1494-1502.

Katafygiotis, L.S., and J.L., Beck, 1998, "Updating Models and Their Uncetainties. II: Model Identifiability", Journal of Engineering Mechanics, Vol. 124. No. 4, pp. 463-467.

Lepage, A., M.W., Hopper, S.A., Delgado, and J., Dragovich, 2010, "Best-fit Models for Nonlinear Seismic Response of Reinforced Concrete Frames", Engineering Structures, No. 32, pp. 2931-2939.

Limongelli, M.P., 2014, "Seismic Health Monitoring of an Instrumented Multistory Building using the Interpolation Method", Earthquake Engineering and Structural Dynamics, Vol. 43, No. 11, pp. 1581-1602.

Liu, K., E., Reynders, G., De Roeck, and G., Lombaert, 2009, "Experimental and Numerical Analysis of a Composite Bridge for High-Speed Trains", Journal of Sound and Vibration, No. 320, pp. 201-220.

Lus, H., R., Betti, and R.W., Longman, 1999, "Identification of Linear Structural Systems Using Earthquake Induced Vibration Data", Earthquake Engineering and Structural Dynamics, No. 28, pp. 1449-1467.

Mackie, K.R., and B., Stojadinovic, 2006, "Post-Earthquake Functionality of Highway Overpass Bridges", Earthquake Engineering and Structural Dynamics, No. 35, pp. 77-93.

Mosquera, V., A.W., Smyth, and R., Betti, 2012, "Rapid Evaluation and Damage Assessment of Instrumented Highway Bridges", Earthquake Engineering and Structural Dynamics, No. 41, pp. 755-774.

Nelson R.B., M., Saiidi, and H., Zadeh 2007, "Experimental Evaluation of Performance of Conventional Bridge Systems. Report No. Cceer-07-04", Center for Earthquake Engineering Research, University of Nevada, Reno, Nv.

Otte, D., P.V.D., Ponseele, and J., Leuridan, 1990, "Operational Shapes Estimation as A Function of Dynamic Loads", In Proceedings of 8th International Modal Analysis Conference, Society for Experimental Mechanics, Orlando, Fl, pp.413–21.

Pankaj, P., and E., Lin, 2005, "Material Modelling in the Seismic Response Analysis for the Design of RC Framed Structures, Engineering Structures, No. 27, pp. 1014-1023.

Park, Y-J., A.H-S, Ang and Y.K., Wen, 1985, "Seismic Damage Analysis of Reinforced Concrete Buildings", Journal of Structural Engineering ASCE, Vol. 111, No. 4, pp. 740-757.

Perry, M.J., and C. G., Koh, 2008, "Output-only Structural Identification in Time Domain: Numerical and Experimental Studies", Earthquake Engineering and Structural Dynamics, No. 37, pp. 517-533.

Phares, B.M., G.A., Washer, D.D., Rolander, B.A., Gaybeal, and M., Moore, 2004, "Routine Highway Bridge Inspection Condition Documentation Accuracy and Reliability", Journal of Bridge Engineering, Vol. 9 No. 4, pp. 403-413.

Priestley, M.J.N., F., Seible and G.M., Calvi, 1996, "Seismic Design and Retrofit of Bridges", Wiley, New York.

Reynders, E., G., Wrusten, and G., De Roeck, 2014, "Output-only Structural Health Monitoring in Changing Environmental Conditions by Means of Nonlinear System Identification", Structural Health Monitoring, Vol. 13, No. 1, pp. 82-93.

Shattarat, N.K., M.D., Symans, D.I., McLean, and W.F., Cofer, 2008, "Evaluation of Nonlinear Static Analysis Methods and Software Tools for Seismic Analysis of Highway Bridges", Engineering Structures, No. 30, pp. 1335-1345.

Shinozuka, M. M.Q., Feng and H-K., Kim, 2000, "Nonlinear Static Procedure for Fragility Curve Development", Journal of Engineering Mechanics vol. 126, No. 12, pp. 1287-1295.

Shinozuka, M., M.Q., Feng, J., Lee and T., Naganuma, 2000, "Statistical Analysis of Fragility Curves", Journal of Engineering Mechanics, Vol. 126, No. 12, pp. 1224-1231.

Shinozuka, M. and R., Ghanem, 1995, "Structural-System Identification. 2: Experimental Verification", Journal of Engineering Mechanics, Vol. 121, No. 2, pp. 265-273.

Singhal, A. and A.S., Kiremidjian, 1998, "Bayesian Updating of Fragilities with Application to RC Frames", Journal of Structural Engineering ASCE, Vol. 124, No. 8, pp. 922-929.

Sohn, H., M., Dzwonczyk, E.G., Straser, A.S., Kiremidjian, K.H., Law, and T., Meng, 1999, "An Experimental Study of Temperature Effect on Modal Parameters of the Alamosa Canyon Bridge", Earthquake Engineering and Structural Dynamics, No. 28, pp. 879-897.

Sohn, H., C.R., Farrar, F.M., Hemez, D.D., Shunk, D.W., Stinemates, B.R., Nadler and J.J., Czarnecki, 2004, "A Review of Structural Health Monitoring Literature", Los Alamos National Laboratory Report, LA-13976-MS.

Soyoz, S., and M.Q., Feng, 2009, "Long-Term Monitoring and Identification of Bridge Structural Parameters", Computer-Aided Civil and Infrastructure Engineering, No. 24, pp. 82-92.

Teughels, A., and G., De Roeck, 2004, "Structural Damage Identification of the Highway Bridge Z24 by FE Model Updating", Journal of Sound and Vibration, No. 278, pp. 589-610.

Xia, P.Q., and J.M.W., Brownjohn, 2004, "Bridge Structural Condition Assessment Using Systematically Validated Finite-Element Model", Journal of Bridge Engineering, Vol.9, No. 5, pp. 418-423.

Westgate, R., K.Y., Koo, J.M.W., Brownjohn, and List, D., 2014, "Suspension Bridge Response due to Extreme Vehicle Loads", Structure and Infrastructure Engineering: Maintenance, Vol. 10, No. 6, pp. 821-833.

Yazgan, U., and A., Dazio 2011, "Simulating Maximum and Residual Displacements of RC Structures: I. Accuracy", Earthquake Spectra, Vol. 27, No. 4, pp. 1187–1202.

Yazgan, U., and A., Dazio 2011, "Simulating Maximum and Residual Displacements of RC Structures: II. Sensitivity", Earthquake Spectra, Vol. 27, No. 4, pp. 1203–1218.

Zhang, Z., C.G., Koh, and M.J., Perry, 2012, "Frequency Domain Sub-Structural Identification for Arbitrary Excitations", Earthquake Engineering and Structural Dynamics, No. 41, pp. 605-621.